AD-A094 020 SYSTEMS AND APPLIED SCIENCES CORP RIVERDALE MD F/G 4/2
COMPUTER-BASED WEATHER RESEARCH.(U)
FEB 80 A M GERLACH F19628-79-C-0033
UNCLASSIFIED AFGL-TR-80-0069 NL

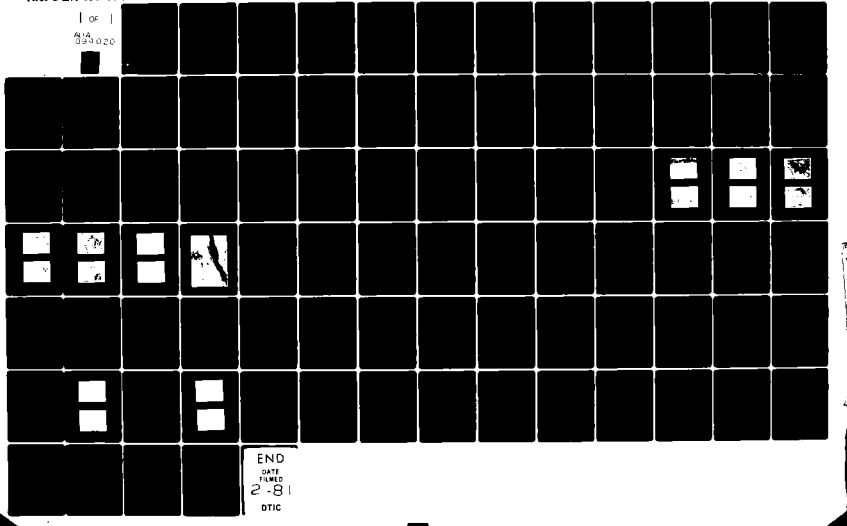

LEVEL II (12)

AFGL-TR-80-0069

AD A094020

COMPUTER-BASED WEATHER RESEARCH

Alan M. Gerlach (ed.)

Systems and Applied Sciences Corporation
6811 Kenilworth Avenue
Riverdale, Maryland 20840

29 February 1980

Scientific Report No. 2

AIR FORCE GEOPHYSICS LABORATORY
AIR FORCE SYSTEMS COMMAND
UNITED STATES AIR FORCE
HANSCOM AFB, MASSACHUSETTS 01731

UNCLASSIFIED

SECURITY CLASSIFICATION OF THIS PAGE (When Data Entered)

REPORT DOCUMENTATION PAGE	READ INSTRUCTIONS BEFORE COMPLETING FORM
1. REPORT NUMBER: AFGL-TR-80-0069	2. GOVT ACCESSION NO.: AD-A094 020
3. RECIPIENT'S CATALOG NUMBER	
4. TITLE (and Subtitle): COMPUTER-BASED WEATHER RESEARCH	5. TYPE OF REPORT & PERIOD COVERED: Scientific Report, No. 2; 1 Dec 78 — 30 Nov 79
6. PERFORMING ORG. REPORT NUMBER	
7. AUTHOR: Alan M. Gerlach (ed.)	8. CONTRACT OR GRANT NUMBER(s): F19628-79-C-0033
9. PERFORMING ORGANIZATION NAME AND ADDRESS: Systems and Applied Sciences Corporation, 6811 Kenilworth Avenue, Riverdale, Maryland 20840	10. PROGRAM ELEMENT, PROJECT, TASK AREA & WORK UNIT NUMBERS: 61102F, 62101F; 667000AA
11. CONTROLLING OFFICE NAME AND ADDRESS: Air Force Geophysics Laboratory, Hanscom AFB, MA 01731, Manager/Charles Burger/LY	12. REPORT DATE: 29 February 1980
	13. NUMBER OF PAGES: 84
14. MONITORING AGENCY NAME & ADDRESS (if different from Controlling Office)	15. SECURITY CLASS. (of this report): UNCLASSIFIED
	15a. DECLASSIFICATION DOWNGRADING SCHEDULE

16. DISTRIBUTION STATEMENT (of this Report)

Approved for public release; distribution unlimited

17. DISTRIBUTION STATEMENT (of the abstract entered in Block 20, if different from Report)

18. SUPPLEMENTARY NOTES

19. KEY WORDS (Continue on reverse side if necessary and identify by block number)

PRIMITIVE EQUATION MODEL
FORECAST ACCURACY
SPATIAL RESOLUTION
WIND SETS
INTERACTIVE FORECASTING
MESOSCALE FORECASTING
ALBEDO
CLOUD BRIGHTNESS

20. ABSTRACT (Continue on reverse side if necessary and identify by block number)

This report details meteorological research conducted by Systems and Applied Sciences Corporation in several areas: development of a limited-area Numerical Weather Prediction model; comparative test of wind sets; development of mesoscale forecasting software for McIDAS; improvement in satellite data brightness analysis techniques. Also, McIDAS hardware and software capabilities were upgraded and used to support field research activities.

DD FORM 1 JAN 73 1473

UNCLASSIFIED

SECURITY CLASSIFICATION OF THIS PAGE (When Data Entered)

FOREWORD

This interim scientific report details the results and status of certain research performed by Systems and Applied Sciences Corporation (SASC) under Contract No. F19628-79-C-0033 for the period December 1, 1978 - November 30, 1979. Presentations vary in technical detail according to their subject matter.

Reports were prepared by the scientists, engineers, and programmers identified in the Table of Contents with their respective technical reports.

TABLE OF CONTENTS

A. DEVELOPMENT OF A LIMITED-AREA NUMERICAL WEATHER PREDICTION MODEL

I. INTRODUCTION

Numerical Weather Prediction (NWP) models of various forms have been used operationally in the United States for about 25 years. Their increased sophistication and complexity have paralleled that of the high-speed computers on which they are implemented. They have developed from the simple equivalent barotropic model, which used various simplifying assumptions to predict the height of the 500 mb pressure surface, to the seven-layer primitive equation model currently in use by the National Meteorological Center (NMC).

Models have developed in complexity as a result of attempts to account more adequately for the various physical processes which significantly affect weather changes. One way is by numerical integration of the so-called "primitive equations"; that is, the spatial and temporal mathematical relationships in their basic form with as few simplifying assumptions as possible, which describe atmospheric behavior. Because of computational storage and time requirements, the equations are integrated in time over a spatial network of grid points of limited resolution in both the horizontal and vertical. Since, however, many important physical processes have spatial scales smaller than the computational grid interval, they cannot be properly accounted for by the system of approximate equations. In addition, the larger the grid spacing, the greater the error associated with the finite difference techniques used in solving the nonlinear partial differential primitive equations.

On the other hand, the observed data used to provide initial and boundary values for the model are available only at a density prescribed by the density of the observational network. Some information may be added or lost by interpolation to accommodate a grid of finer resolution. There-

fore it is not certain that integration of the [illegible] tions over grids of increasingly finer resolution would [illegible] increasingly better forecasts. [illegible] ment in the forecast gained in this way may [illegible] significant enough to justify the [illegible] costs involved. For example, [illegible] the mesh without changing the [illegible] require a fourfold increase in computer [illegible] eightfold increase in auxiliary [illegible] fold increase in computer power ([illegible], 19[illegible]).

The purpose of this report [illegible] dimensional NWP model in which [illegible] speed and accuracy of forecasts [illegible] by the horizontal resolution. The [illegible] time integration of the primitive equations [illegible] various horizontal resolution for a [illegible] area of the earth, and for the total [illegible] resolved into six layers for which [illegible]. [illegible] goal is ultimately to determine the [illegible] tion for a given input in the initial [illegible] tions in order that prediction [illegible] computational speed [illegible] efficiency maximized.

II. DESCRIPTION OF THE MODEL

In studying the relationship between [illegible] and spatial resolution in NWP models, it was [illegible] simple to use a proven primitive [illegible] produced acceptable forecasts. Therefore the [illegible] of the six-layer NMC Limited-Area Fine Mesh (LFM) model was used in formulating the variable resolution model in this study. Design of the model was [illegible] Shuman and Hovermale (1968); complete documentation of the operational model was written by [illegible] (19[illegible]). [illegible] explanation of the LFM model will be limited to the [illegible] theory involved in the model.

Values of the prognostic variables are [illegible]

of the hydrostatic meteorological equations, given here in Cartesian form on a conformal projection of the earth:

$$\frac{\partial}{\partial t}\left(\frac{u}{m}\right) = \frac{v}{m}\left\{f + m^2\left[\frac{\partial}{\partial x}\left(\frac{v}{m}\right) - \frac{\partial}{\partial y}\left(\frac{u}{m}\right)\right]\right\} - \frac{\partial \Phi}{\partial x} - c_p\theta\frac{\partial \pi}{\partial x} - \dot{\sigma}\frac{\partial}{\partial \sigma}\left(\frac{u}{m}\right) - \frac{\partial}{\partial x}\left[\frac{u^2 + v^2}{2}\right] - F_x \quad (1)$$

$$\frac{\partial}{\partial t}\left(\frac{v}{m}\right) = -\frac{u}{m}\left\{f + m^2\left[\frac{\partial}{\partial x}\left(\frac{v}{m}\right) - \frac{\partial}{\partial y}\left(\frac{u}{m}\right)\right]\right\} - \frac{\partial \Phi}{\partial y} - c_p\theta\frac{\partial \pi}{\partial y} - \dot{\sigma}\frac{\partial}{\partial \sigma}\left(\frac{v}{m}\right) - \frac{\partial}{\partial y}\left[\frac{u^2 + v^2}{2}\right] - F_y \quad (2)$$

$$\frac{\partial}{\partial t}\left(\frac{\partial p}{\partial \sigma}\right) = -m^2\left[\frac{\partial}{\partial x}\left(\frac{u}{m}\frac{\partial p}{\partial \sigma}\right) + \frac{\partial}{\partial y}\left(\frac{v}{m}\frac{\partial p}{\partial \sigma}\right)\right] - \frac{\partial}{\partial \sigma}\left(\dot{\sigma}\frac{\partial p}{\partial \sigma}\right) \quad (3)$$

$$\frac{\partial \theta}{\partial t} = -m\left[u\frac{\partial \theta}{\partial x} + v\frac{\partial \theta}{\partial y}\right] - \dot{\sigma}\frac{\partial \theta}{\partial \sigma} + H \quad (4)$$

$$\frac{\partial W}{\partial t} = -m^2\left[\frac{\partial}{\partial x}\int_{\sigma_U}^{\sigma_L}\frac{\alpha W u}{m}\,d\sigma + \frac{\partial}{\partial y}\int_{\sigma_U}^{\sigma_L}\frac{\alpha W v}{m}\,d\sigma\right] - \left[\alpha W \dot{\sigma}\right]_{\sigma_U}^{\sigma_L} + C. \quad (5)$$

For this system of equations to comprise a closed set, the following accompanying diagnostic equations were included in the model:

$$\frac{\partial \Phi}{\partial \pi} = -c_p\theta \quad (6)$$

$$\pi = \left(\frac{p}{P}\right)^{R/c_p} \quad (7)$$

$$\frac{\partial p}{\partial \sigma}\frac{\partial^2 \dot{\sigma}}{\partial \sigma^2} = -m^2\left[\frac{\partial}{\partial x}\left(\frac{1}{m}\frac{\partial p}{\partial \sigma}\frac{\partial u}{\partial \sigma}\right) + \frac{\partial}{\partial y}\left(\frac{1}{m}\frac{\partial p}{\partial \sigma}\frac{\partial v}{\partial \sigma}\right)\right]. \quad (8)$$

In these equations x and y are the two horizontal Cartesian coordinates on the projection; t time, u and v the x and y components of velocity true on the earth; θ potential temperature; $\Phi = gz$, geopotential above the projection where g is acceleration due to gravity (taken as constant) and z is height above sea level; p pressure; P, 1,000 mb; R the gas constant for dry air; c_p the specific heat of air at constant pressure; $m = (1 + \sin 60^\circ)/(1 + \sin \phi)$, where ϕ is [illegible] latitude, the map factor of the polar stereo-

graphic projection with 60°N as the standard latitude; f the Coriolis parameter; and W the precipitable water. F_x and F_y are the x and y components of acceleration due to friction and turbulence; H represents diabatic heat influences; and C the rate of gain or loss of water vapor due to evaporation or condensation. Vertical velocity is $\dot{\sigma} = d\sigma/dt$.

Vertical coordinate σ is expressed in the general form

$$\sigma = \frac{p - p_U}{p_L - p_U} \qquad (9)$$

where p_U is the pressure on a given quasi-horizontal surface bounding an atmospheric layer above, p_L the pressure on the surface bounding the layer below, and p the pressure at a point in question within that layer. Coordinate σ is defined differently in each of the four domains, as illustrated in Fig. A-1, which depicts the vertical structure of the model.

The area chosen for consideration in this study is a segment of the NMC octagonal grid which completely includes the contiguous United States. The coarsest resolution used in this study is equal to twice that of the NMC octagonal grid, with grid points 190.5 km apart at 60°N. A grid of 33 x 33 grid points was used over which computations were carried out, with the outermost row designated as the boundary. The model was initially designed to consider only this resolution, but is being modified to accommodate double and four times this resolution in order to accomplish the primary goal of the study.

Numerical solution of the model equations begins with the specification of initial values of prognostic variables u, v, θ, $\partial p/\partial\sigma$, and W. Values of variables u, v, and θ must be specified initially for all seven levels, but θ is held constant in time and space in the uppermost or cap layer. Holding θ constant in this way facilitates use of the cap layer for strictly computational purposes - the values of u, v, and $\partial p/\partial\sigma$ forecast in this domain are used only to obtain values for the variables in the other domains. Initial values for W must be available at all grid points in the lowest three layers only, since it is taken to be

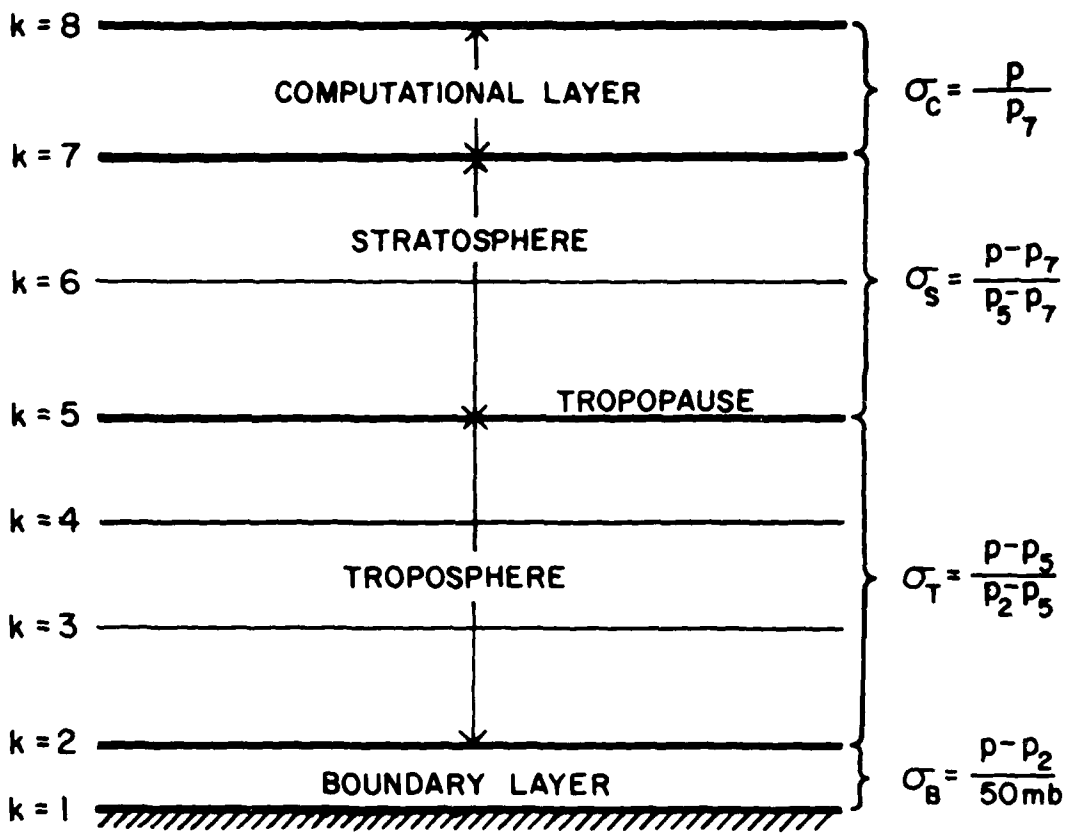

Figure A-1. Schematic diagram of LFM vertical structure.

zero everywhere above. W is obtained in each layer from the initially specified specific humidity q by means of the relationship

$$W = \frac{1}{g}\int_{\sigma_U}^{\sigma_L} q \frac{\partial p}{\partial \sigma}\, d\sigma \qquad (10)$$

where σ_U and σ_L represent top and bottom of the layer in question. Fig. A-2 illustrates the relative locations of the prognostic and diagnostic variable values in each layer.

Once these values are obtained the model determines the pressures p at all grid points on the interfaces between layers by vertically integrating, using values of $\partial p/\partial \sigma$. Since $\partial p/\partial \sigma$ is independent of height in each domain, pressure at each σ interface in each domain is given by the expression

$$p(\sigma) = p(\sigma = 0) + \frac{\partial p}{\partial \sigma}\,\sigma . \qquad (11)$$

With pressure at the top of the model atmosphere set equal to zero, this expression is used to evaluate the pressure at all grid points (with $p_B \equiv p_1 - p_2 = 50$ mb everywhere in the boundary layer). From these values the model obtains values for π from (7), so that (6) may be integrated numerically upward to obtain the values of Φ at all layer interfaces. At this point, (8) is evaluated numerically at all layer interfaces except for the material surfaces designated by k = 1, 5, 7, and 8 (see Fig. A-1) where it is assumed that $\dot{\sigma} = 0$. These assumptions also serve as boundary conditions in solving (8). In addition to these boundary conditions, the boundary condition for $\dot{\sigma}_T$ at the top of the boundary layer

$$\dot{\sigma}_T(\sigma_T = 1) = \frac{p_B}{p_1 - p_B - p_5}\left\{ m^2\left[\frac{\partial}{\partial x}\left(\frac{u_B}{m}\right) + \frac{\partial}{\partial y}\left(\frac{v_B}{m}\right)\right]\right\} \qquad (12)$$

where u_B and v_B are the boundary layer velocity components, is obtained by integrating the boundary layer version of the continuity equation (3) through the depth of the boundary layer and by observing the requirement of mass balance in the total troposphere.

To obtain the predicted value of W for the lowest three layers it is assumed that the vertical variation of q at

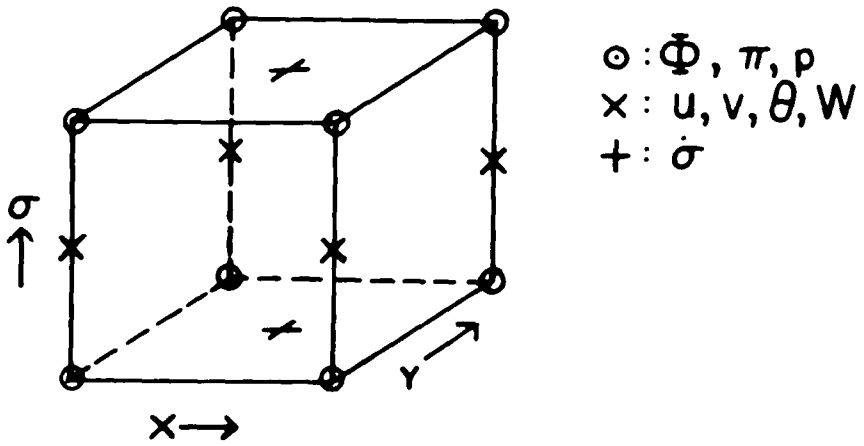

Figure A-2. Schematic diagram depicting a computational cube. In each cube of the three-dimensional matrix of grid points, the quantities are carried at each point in time at their indicated positions.

each grid point is a linear function of pressure through all three layers:

$$q\frac{\partial p}{\partial \sigma} = g\alpha W \qquad (13)$$

where α is the function of σ that will determine the distribution of q. When (13) is substituted into the expression obtained from combining the conservation of specific humidity with (3), the prognostic equation (5) for W is obtained. Values of $\alpha(x,y,\sigma,t)$ in each layer at each time step are obtained by means of the expressions

$$\alpha_B = a_B + b_B\sigma_B$$

$$\alpha_T = a_T + b_T\sigma_T$$

in the boundary layer and two tropospheric layers respectively, where a and b are arbitrary functions of x, y, and t only. These are derived from four simultaneous equations (see Shuman and Hovermale, 1968) and are given by $b_T = 18/(2 + 3c)^2$, $b_B = c^2 b_T$, $a_T = -b_T/3$, and $a_B = 2cb_T/3$ where $c = (\partial p/\partial\sigma)_B/(\partial p/\partial\sigma)_T$.

The model was formulated so as to neglect frictional influences, diabatic heating effects, and changes in total water vapor; thus $F_x = F_y = H = C = 0$. This was done so that the relationship between the basic dynamics of the model and model resolution might be investigated at first without the added complication of these more complex effects. In addition, water vapor concentration has been set initially to zero everywhere, to consider the simplified case of a dry atmosphere. Values of Coriolis parameter and map factor were calculated for all grid points and stored in a form readily accessible by the model. Eventually terrain height, sea surface temperatures, and drag coefficient values for all relevant grid points will be made available to the model. As the model is now formulated, the only one of these parameters necessary is terrain height, which is set equal to zero at all ground surface grid points. Thus, at this point the model has determined all values needed to evaluate the right sides of equations (1)

through (5) as they are currently formulated.

Terms on the right side of the prognostic equations were coded in the model according to a finite difference scheme devised by Shuman and Hovermale (1968). Since different (albeit perfectly acceptable) forms of the finite difference representations of the terms would in general yield substantially different model results, great care was taken to calculate the terms in the model according to the methodology of Shuman and Hovermale. When the finite difference forms of the right side terms are evaluated at their respective grid points at each time step, the model either (1) multiplies their sum by one time interval in seconds and adds this to the initial value of the prognostic variable in question for the first time step, or (2) multiplies their sum by twice the time interval and adds to the value of the prognostic variable at the previous time step for successive time steps. This requires storage of two arrays of values of each of the prognostic variables at each time step, in addition to storage of the values of the diagnostic variables at the present time step. This large data storage requirement prohibited simultaneous storage of all values necessary for calculation of all variables in core memory at the same time. Using mass storage and common array storage within the model and making calculations for each prognostic equation in separate sections of the program greatly reduced core storage requirements.

III. ONE-LAYER VERSION OF LFM

To elucidate the relationship between spatial resolution and accuracy of model results, it is desirable to investigate progressively more complex forms of the model, beginning with its simplest form. It was believed that understanding the effect of change of resolution and finite difference forms of the derivatives at simpler levels of model complexity would facilitate understanding model behavior in its more complex forms. For this reason the three-dimensional model described above was modified to include logical switches allowing simulation of the prognostic variables

u, v, θ, and $\partial p/\partial\sigma$ in one atmospheric layer only. This is equivalent in theory to holding vertical velocity equal to zero everywhere. The one-layer model atmosphere is confined between two material surfaces, so that Φ_1, π_1, p_1 and Φ_2, π_2, p_2 represent the values of these variables at the top and bottom σ surfaces respectively, with $\sigma_1 = 1$, $\sigma_2 = 0$. Prognostic variables u, v, and θ are considered independent of height in the layer, along with $\partial p/\partial\sigma$, which is also height independent in each domain in the multi-layer model.

First model runs were thus based on the assumption of a dry, adiabatic, inviscid, one-layer atmosphere. In addition it was assumed that $\Phi_1 = 0$ everywhere (smooth ground surface) and that $p_2 = 0$ everywhere (top of the layer is top of the atmosphere). With these assumptions the prognostic equations (1) - (4) reduce to the form

$$\frac{\partial}{\partial t}\left(\frac{u}{m}\right) = \frac{v}{m}\left\{f + m^2\left[\frac{\partial}{\partial x}\left(\frac{v}{m}\right) - \frac{\partial}{\partial y}\left(\frac{u}{m}\right)\right]\right\} - \frac{\partial \Phi_2}{\partial x} - c_p\theta\frac{\partial \pi_1}{\partial x} - \frac{1}{2}\frac{\partial}{\partial x}\left\{m^2\left[\left(\frac{u}{m}\right)^2 + \left(\frac{v}{m}\right)^2\right]\right\} \tag{14}$$

$$\frac{\partial}{\partial t}\left(\frac{v}{m}\right) = -\frac{u}{m}\left\{f + m^2\left[\frac{\partial}{\partial x}\left(\frac{v}{m}\right) - \frac{\partial}{\partial y}\left(\frac{u}{m}\right)\right]\right\} - \frac{\partial \Phi_2}{\partial y} - c_p\theta\frac{\partial \pi_1}{\partial y} - \frac{1}{2}\frac{\partial}{\partial y}\left\{m^2\left[\left(\frac{u}{m}\right)^2 + \left(\frac{v}{m}\right)^2\right]\right\} \tag{15}$$

$$\frac{\partial}{\partial t}\left(\frac{\partial p}{\partial \sigma}\right) = -m^2\left[\frac{\partial}{\partial x}\left(\frac{u}{m}\frac{\partial p}{\partial \sigma}\right) + \frac{\partial}{\partial y}\left(\frac{v}{m}\frac{\partial p}{\partial \sigma}\right)\right] \tag{16}$$

$$\frac{\partial \theta}{\partial t} = -m^2\left[\left(\frac{u}{m}\right)\frac{\partial \theta}{\partial x} + \left(\frac{v}{m}\right)\frac{\partial \theta}{\partial y}\right] \tag{17}$$

with the diagnostic equations $\Phi_2 = c_p\theta\pi$, $\sigma(p) = p/p_1$, $\partial p/\partial\sigma = p_1$, and $\pi_1 = (p_1/P)^{R/c_p}$. The modified one-layer version of the model numerically integrates the finite difference form of these equations over the 33 x 33 grid point grid lattice using six-minute time steps. Initial and boundary values for the four prognostic variables used to obtain the numerical solutions to these equations will be discussed below.

In addition to this general one-layer version of the model, two simpler versions were formulated by the succes-

sive incorporation of these assumptions:

(1) Incompressible motion (assume $\partial p/\partial\sigma$ = 1,000 mb in time and space). Model equations take the form

$$\frac{\partial}{\partial t}\left(\frac{u}{m}\right) = \frac{v}{m}\left\{f + m^2\left[\frac{\partial}{\partial x}\left(\frac{v}{m}\right) - \frac{\partial}{\partial y}\left(\frac{u}{m}\right)\right]\right\} - \frac{\partial \Phi_2}{\partial x} - \tfrac{1}{2}\frac{\partial}{\partial x}\left\{m^2\left[\left(\frac{u}{m}\right)^2 + \left(\frac{v}{m}\right)^2\right]\right\} \tag{18}$$

$$\frac{\partial}{\partial t}\left(\frac{v}{m}\right) = -\frac{u}{m}\left\{f + m^2\left[\frac{\partial}{\partial x}\left(\frac{v}{m}\right) - \frac{\partial}{\partial y}\left(\frac{u}{m}\right)\right]\right\} - \frac{\partial \Phi_2}{\partial y} - \tfrac{1}{2}\frac{\partial}{\partial y}\left\{m^2\left[\left(\frac{u}{m}\right)^2 + \left(\frac{v}{m}\right)^2\right]\right\} \tag{19}$$

$$\frac{\partial}{\partial x}\left(\frac{u}{m}\right) + \frac{\partial}{\partial y}\left(\frac{v}{m}\right) = 0 \tag{20}$$

$$\frac{\partial \theta}{\partial t} = -m^2\left[\left(\frac{u}{m}\right)\frac{\partial \theta}{\partial x} + \left(\frac{v}{m}\right)\frac{\partial \theta}{\partial y}\right] \tag{21}$$

where $\Phi_2 = c_p\theta$.

(2) Incompressible, inertial motion (assume $\partial p/\partial\sigma$ = 1,000 mb and θ = 250°K in time and space). In this case the model integrates the equations

$$\frac{\partial}{\partial t}\left(\frac{u}{m}\right) = \frac{v}{m}\left\{f + m^2\left[\frac{\partial}{\partial x}\left(\frac{v}{m}\right) - \frac{\partial}{\partial y}\left(\frac{u}{m}\right)\right]\right\} - \tfrac{1}{2}\frac{\partial}{\partial x}\left\{m^2\left[\left(\frac{u}{m}\right)^2 + \left(\frac{v}{m}\right)^2\right]\right\} \tag{22}$$

$$\frac{\partial}{\partial t}\left(\frac{v}{m}\right) = -\frac{u}{m}\left\{f + m^2\left[\frac{\partial}{\partial x}\left(\frac{v}{m}\right) - \frac{\partial}{\partial y}\left(\frac{u}{m}\right)\right]\right\} - \tfrac{1}{2}\frac{\partial}{\partial y}\left\{m^2\left[\left(\frac{u}{m}\right)^2 + \left(\frac{v}{m}\right)^2\right]\right\} \tag{23}$$

$$\frac{\partial}{\partial x}\left(\frac{u}{m}\right) + \frac{\partial}{\partial y}\left(\frac{v}{m}\right) = 0. \tag{24}$$

These assumptions were individually incorporated into the model by means of logical switches which excluded terms that were affected by the respective assumptions.

Initial and boundary values used for all forms of the one-layer version of LFM were derived from a spatial, temporal stream function which is a solution to the equation expressing the conservation of absolute vorticity. This equation is obtained from the system of equations describing two-dimensional, incompressible motion on the surface of a sphere:

$$\frac{\partial u}{\partial t} = -\frac{u}{a\cos\phi}\frac{\partial u}{\partial \lambda} - \frac{v}{a}\frac{\partial u}{\partial \phi} - \frac{1}{a\cos\phi}\frac{\partial \phi}{\partial \lambda} + v\left(f + \frac{u}{a}\tan\phi\right) \quad (25)$$

$$\frac{\partial v}{\partial t} = -\frac{u}{a\cos\phi}\frac{\partial v}{\partial \lambda} - \frac{v}{a}\frac{\partial v}{\partial \phi} - \frac{1}{a}\frac{\partial \phi}{\partial \phi} - u\left(f + \frac{u}{a}\tan\phi\right) \quad (26)$$

$$\frac{1}{a\cos\phi}\left(\frac{\partial u}{\partial \lambda} + \frac{\partial (v\cos\phi)}{\partial \phi}\right) = 0 \quad (27)$$

where λ represents longitude and ϕ latitude. The motion governed by these equations conserves absolute vorticity, $\xi + f$, where $\xi = (a\cos\phi)^{-1}\ \partial v/\partial\lambda - \partial(u\cos\phi)/\partial\phi$ is the relative vorticity. This can be shown by cross differentiating (25) and (26) and subtracting the resulting form of (25) from that of (26) and by observing that the motion field is non-divergent as stated by (27). The result is the expression for conservation of absolute vorticity:

$$\frac{\partial}{\partial t}(\xi + f) = -\frac{u}{a\cos\phi}\frac{\partial}{\partial \lambda}(\xi + f) - \frac{v}{a}\frac{\partial}{\partial \phi}(\xi + f). \quad (28)$$

Because the motion field is non-divergent as specified by (27) the motion field $\vec{V}$ can be expressed in the form of a stream function ψ such that $\vec{V} = \vec{k} \times \vec{\nabla}_s \psi$, where $\vec{k}$ is the unit vector normal to the spherical surface and $\vec{\nabla}_s = (a\cos\phi)^{-1}\vec{i}\,\partial/\partial\lambda + a^{-1}\vec{j}\,\partial/\partial\phi$, with $\vec{i}$ and $\vec{j}$ representing unit vectors directed along latitude and longitude lines respectively. Thus $u = -a^{-1}\partial\psi/\partial\phi$, $v = (a\cos\phi)^{-1}\partial\psi/\partial\lambda$, and $\xi = \nabla_s^2\psi$. When these expressions are substituted in (28) it can be verified that a stream function of the general form

$$\psi(\phi, \lambda, t) = A(t)P_n^m(\sin\phi)\,e^{im\lambda} \quad (29)$$

is a solution to the resulting equation, where $A = A_0 \exp\{im2\Omega t/n(n+1)\}$ in which A_0 is an arbitrary initial amplitude and Ω is the earth's rotation rate in sec^{-1}, and $P_n^m(\sin\phi)$ is the associated Legendre function of degree n and order m. This travelling wave solution to the vorticity equation (28) is known as the Rossby-Haurwitz Wave, where m and n specify zonal and meridional numbers respectively. Initial and boundary values for u and v in all versions of the one-layer model were derived from this stream function

for the case m = 2, n = 3, and were transformed from spherical to Cartesian coordinates.

In all but the case of incompressible, inertial motion, initial and boundary values of potential temperature θ were required. These were obtained in the following manner. It was first determined that if the motion dictated by equations (25) - (27) was to be confined to two dimensions (i.e., to the surface of the sphere), the motion field must not only be initially non-divergent, but that the divergence tendency must also be zero everywhere in the motion field in order to conserve mass. This additional constraint is used with equations (25) - (27) to obtain the balance equation

$$\nabla_s^2 \Phi = 2\left[\left(\frac{1}{a\cos\phi}\frac{\partial u}{\partial\lambda}\right)\left(\frac{1}{a}\frac{\partial v}{\partial\phi}\right) - \left(\frac{1}{a\cos\phi}\frac{\partial v}{\partial\lambda}\right)\left(\frac{1}{a}\frac{\partial u}{\partial\phi}\right)\right] + \xi f - \frac{u}{a}\frac{\partial f}{\partial\phi} - \left(\frac{u^2+v^2}{a^2}\right) - 2\left[\frac{1}{a}\frac{\partial u}{\partial\phi}\frac{u\tan\phi}{a} + \frac{1}{a}\frac{\partial v}{\partial\phi}\frac{v\tan\phi}{a}\right] \qquad (30)$$

which expresses the relationship that must exist between the geopotential field and the motion field to insure that the motion field is instantaneously and temporally non-divergent (i.e., in "balance" with the geopotential field at all times). By substituting (29) in this expression one obtains the relationship between geopotential field and stream function with which it is in balance. Geopotential field $\Phi(\phi, \lambda, t)$ that satisfies this equation was expressed as a linear combination of spherical harmonics. By noticing from (16) that non-divergent motion is equivalent to holding $\partial p/\partial\sigma$ (and thus π_1) constant everywhere in the layer, potential temperature was obtained from the balanced geopotential by the expression $\theta = \Phi_2/c_p$, where $\Phi_2 = 2\Phi(\phi, \lambda, t)$ from the assumption that Φ in the middle of the layer is a simple average of the values of geopotential at the top and bottom of the layer. In this way initial and boundary values of θ (which are in balance with initial and boundary values of u and v) were obtained. Since initial and boundary motions are non-divergent, initial and boundary

values for $\partial p/\partial\sigma$ were held constant at a value of 1,000 mb.

While balance is maintained in the initial and boundary values of u, v, and θ throughout time, no such guarantee of instantaneous and temporal non-divergence exists for any of the forms of the one-layer model equations. The balance equation is not used in the model to insure such a balance. In the simplest case of incompressible, inertial motion, a divergent residual remains when the right side of (22) and (23) are evaluated using the non-divergent initial motion field. In the other two cases of the one-layer model, potential temperature is calculated according to the conservation of potential temperature and not according to the balance equation, with no assurance of a balance between Φ and u,v. Hence results from any form of the one-layer model would not in general be non-divergent, while the initial and boundary motions used in the model are strictly non-divergent at all times. As the magnitude of the divergent component in the interior motion field grows, it will become more and more unlike the non-divergent boundary motions, and discontinuities may arise at the interface between the interior and boundaries of the motion field. However, the balanced motion and temperature fields will be used as initial and boundary values until values more compatible with the interior can be found.

A smoothing operator was also incorporated into a separate version of the model. It is applied to all prognostic variables at each time step, and is identical to that used by NMC as described by Gerrity and Newell (1976). The smoother is a 25-point operator at all points two or more grid intervals from the boundary and a nine-point operator at points only one interval from the boundary.

IV. CURRENT STATUS OF IFM MODEL DEVELOPMENT AND PLANS

Some preliminary model runs have been conducted with all three versions of the one-layer model. The earliest runs consisted primarily of efforts to debug the model, with only the most recent runs yielding results which accurately represent the dynamics of the model equations.

Computer codes are currently being written to present results in graphical form so they may be more easily interpreted.

Outputs from the three versions of the one-layer model will be analyzed and compared against each other to determine the effect of each set of assumptions. The truncation error of the numerical finite difference scheme will be analyzed by numerically computing the terms on the right side of the momentum equations using the Rossby-Haurwitz velocity field values and comparing these against analytic values for the terms. A more accurate fourth-order accuracy finite difference scheme will be devised and implemented in the one-layer model in order to determine the role of the finite difference scheme in forecast accuracy. Its values for the momentum equation terms will also be compared against their analytic values using Rossby-Haurwitz values. The model will be further modified to accommodate doubling and quadrupling the horizontal resolution, as well as to include more complex physical processes as friction, diabatic heating, topography, and water phase changes. The model will also be expanded vertically to include computations for the entire vertical extent of the model atmosphere as shown in Fig. A-1.

V. REFERENCES

Balint, Francis J., 1978: Modeling the weather. Datamation, May 1978, 131-140.

Gerrity, Joseph P., Jr., 1977: The LFM Model - 1976: A documentation. National Meteorological Center, NOAA Technical Memorandum NWS, NMC 60.

-----, and J. E. Newell, 1976: A note on the LFM time integration. NOAA, National Weather Service, National Meteorological Center, Office Note 129.

Shuman, F. G., and J. B. Hovermale, 1968: An operational six-layer primitive equation model. J. Applied Meteor., 7, 525-547.

B. A COMPARATIVE STUDY OF WIND SETS FOR AUTOMATED WEATHER SYSTEMS

I. INTRODUCTION

A primary goal of the Air Force's research and development program is to develop automated weather observing systems which will function unattended in an all-weather environment. As a step toward achieving this goal, a study is underway to examine four wind sets and their response characteristics under a variety of weather conditions.

The four instruments being tested are the Rosemount Orthogonal Airspeed System, the Climatronics Wind System - Mark I, the R. M. Young Propvane, and the J-Tec Vortex Anemometer. Based on AFGL's extensive prior experience with, and confidence in, the Climatronics Wind System - Mark I, it is being used as the standard of comparison in the study.

II. DESCRIPTION OF INSTRUMENTS

The four wind instruments were selected because each makes use of a different principle for determining wind speed or direction. The J-Tec VA-300 Vortex Anemometer consists of a fiberglass wind vane which determines wind direction through the use of a potentiometer. Mounted on the wind direction vane is an obstacle which creates a series of vortices in the downstream flow. These vortices are detected by an ultrasonic beam, their frequency is determined and is converted to wind speed. The instrument was designed for unattended operation in a high-wind environment.

The Climatronics Wind System - Mark I has been used in a number of mesoscale weather field studies and in the Modular Automated Weather System (MAWS) demonstration at Scott AFB. It consists of a set of stainless steel cups

which, in response to wind, rotate and cause a light source to be chopped at a frequency which is proportional to the speed. The wind direction is determined by a vane which is connected to a frictionless direction transducer.

The R. M. Young Propvane Model 8002C consists of a wind vane, which determines wind direction by use of a potentiometer, coupled with a propeller, which activates a D.C. generator whose voltage output is directly proportional to wind speed.

The Rosemount Model 853 Orthogonal Airspeed System measures two orthogonal wind speed vectors of air flow. The instrument has no moving parts. Instead, pressure ports located on the sensor's cylindrical body develop differential pressures which are proportional to the wind speed. Resolution of these pressure differentials through a transducer allows the computation of wind direction and speed.

III. WEATHER TEST FACILITY

The test is being conducted at the AFGL Weather Test Facility at Otis AFB, MA. The facility was designed primarily to serve as a test-bed for the comparison of new sensors for Air Force use and for the examination of weather automation. It was felt that the wide variety of weather that occurs in this area would provide an excellent environment in which to test the durability and responsiveness of the candidate wind sets. Fig. B-1 shows the instrumented towers A, B, C, P, and Q, and the ground site X, where the wind sets are installed.

The Modular Automated Weather System is also located at the Weather Test Facility and is connected to Hanscom AFB by commercial telephone lines. At the base of each tower and at the ground site (see Fig. B-1) a remote data unit (RDU) is located. These RDU's serve as links between the weather sensors and the MAWS data acquisition system.

The RDU's are microprocessors which poll the sensors, convert the analog signals to digital, sum the values, and produce a one-minute mean for each sensor. Included are

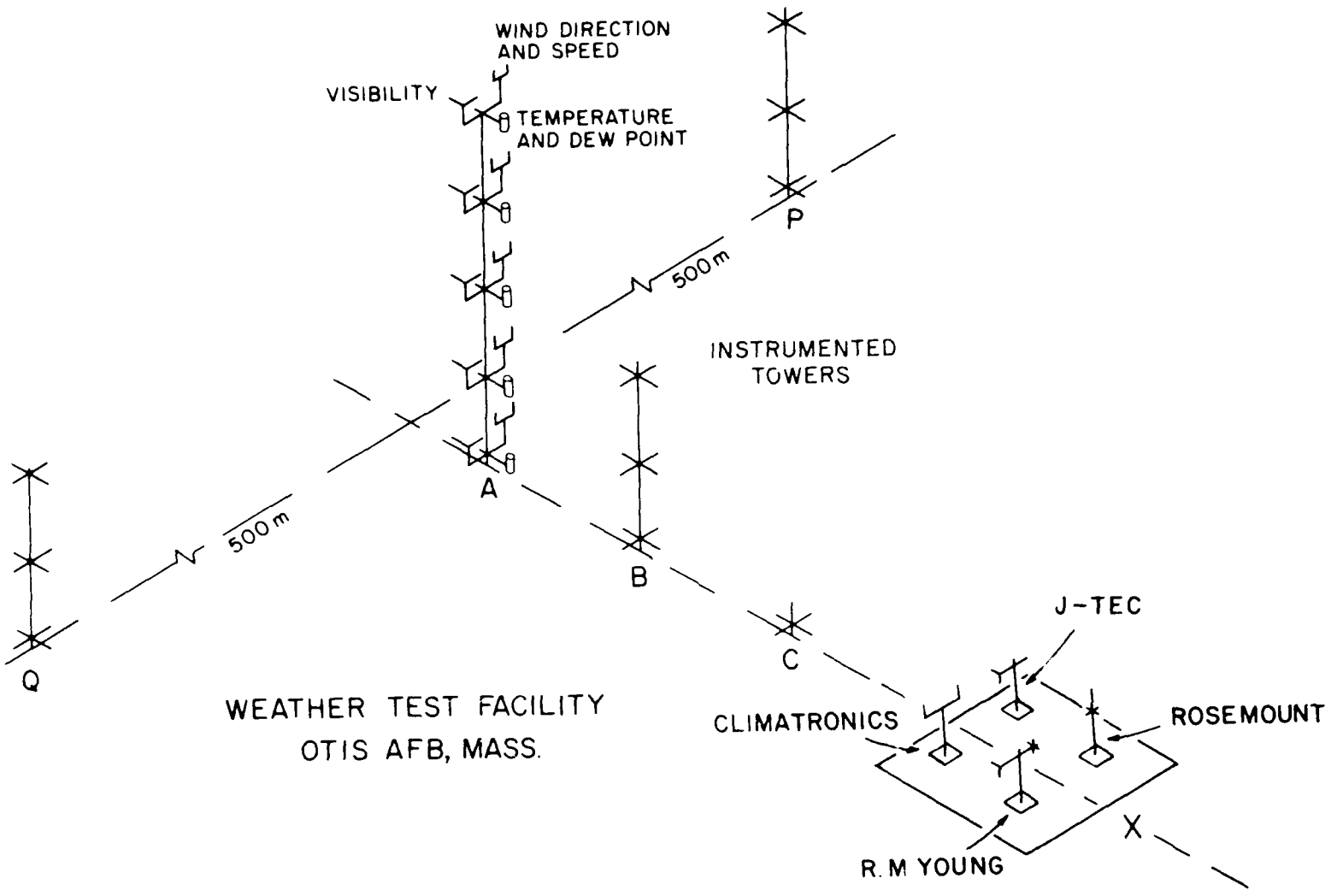
WIND DIRECTION
AND SPEED
VISIBILITY
TEMPERATURE
AND DEW POINT
P
500m
INSTRUMENTED
TOWERS
A
B
C
500m
Q
J-TEC
CLIMATRONICS
ROSEMOUNT
R.M YOUNG
X
WEATHER TEST FACILITY
OTIS AFB, MASS.

Figure B-1.

visibility instruments such as scatter meters, transmissometers, videograph, and nephelometer; and other instruments such as the wind sets described in Section II, radiometers, temperature and dewpoint sensors, rain gauge, and rotating beam ceilometers.

Most sensors report at 12-second intervals; the wind sets report each six seconds. Data from the RDU's are fed to a supervisor at the rate of 120 characters per second for further processing. Refined means, collected from all activated sensors, or the raw voltages from up to 20 selected sensors, are sent to AFGL for real-time print display or archiving on magnetic tape.

A CDC 6600 computer program has been developed to process data from these magnetic tapes to form a data base for several research projects, including cloud base height studies and wind shear investigations. In the case of the wind data, one-minute mean u, v components are calculated, from which the resultant one-minute mean wind direction and speed are obtained. The one exception to this procedure are the data from the Rosemount Orthogonal Airspeed System, which are initially obtained in u, v component form.

IV. DATA ANALYSIS

Software has been developed to analyze the data collected by the four wind sets. Two correlation programs were written. The first, which is executed as part of the routine analysis of the Otis data, compares the wind direction and wind speed from the wind sets by means of scatter diagrams. In the comparison of the Rosemount with the Climatronics, three wind speed regimes (wind speed greater than 4.0 m/sec, greater than 2.5 m/sec, and all wind speeds) are evaluated due to known characteristics of the Rosemount. The scatter program also compares the J-Tec and the R. M. Young with the Climatronics, using the all-wind-speed category. In addition to the computer-printed scatter plots, calculations are made which give the equation of best fit, the RMS error, the correlation,

an average of each variable, the standard deviations, the co-variance, and the standard error of estimate.

The second program produces a pen and ink plot of the scatter diagrams, as illustrated in Figs. B-2 through B-5. Information displayed on the plots consists of the date-time group (e.g., 6 September 1979), the number of observations (N), and the equation of the line of best fit. These figures are provided to illustrate how the scatter diagram analysis is being used in the evaluation of the four wind sensors. Fig. B-2 shows that the J-Tec wind speed is consistently higher than the Climatronics; therefore, recalibration of the voltage-to-wind speed algorithm would be required. However, the relationship is linear and there is very little scatter. The wind direction comparison (Fig. B-3) covers a small range of direction but the fit is excellent. The wind speed comparison between the Climatronics and the R. M. Young (Gill) (Fig. B-4) shows that the R. M. Young consistently reports lower speeds than the Climatronics, and again algorithm adjustment is in order, but the relationship is linear and the scatter is quite small. The wind direction comparison between the two (Fig. B-5) is very good. In the later phases of the study, after a sufficiently large data set has been accumulated, the calibration algorithms will be adjusted prior to the comparison based on weather conditions.

In order to compare the wind sets in different weather conditions, use will also be made of a decision-tree computer program developed for another project. The decision-tree program, using data from the automated instrument array at Otis, objectively determines the kinds of weather and obstructions to vision that are occurring. Fig. B-6 lists the elements normally observed by human observers and indicates those which the decision-tree program has the ability to specify. This program is being used to classify the periods during which the wind sets will be compared.

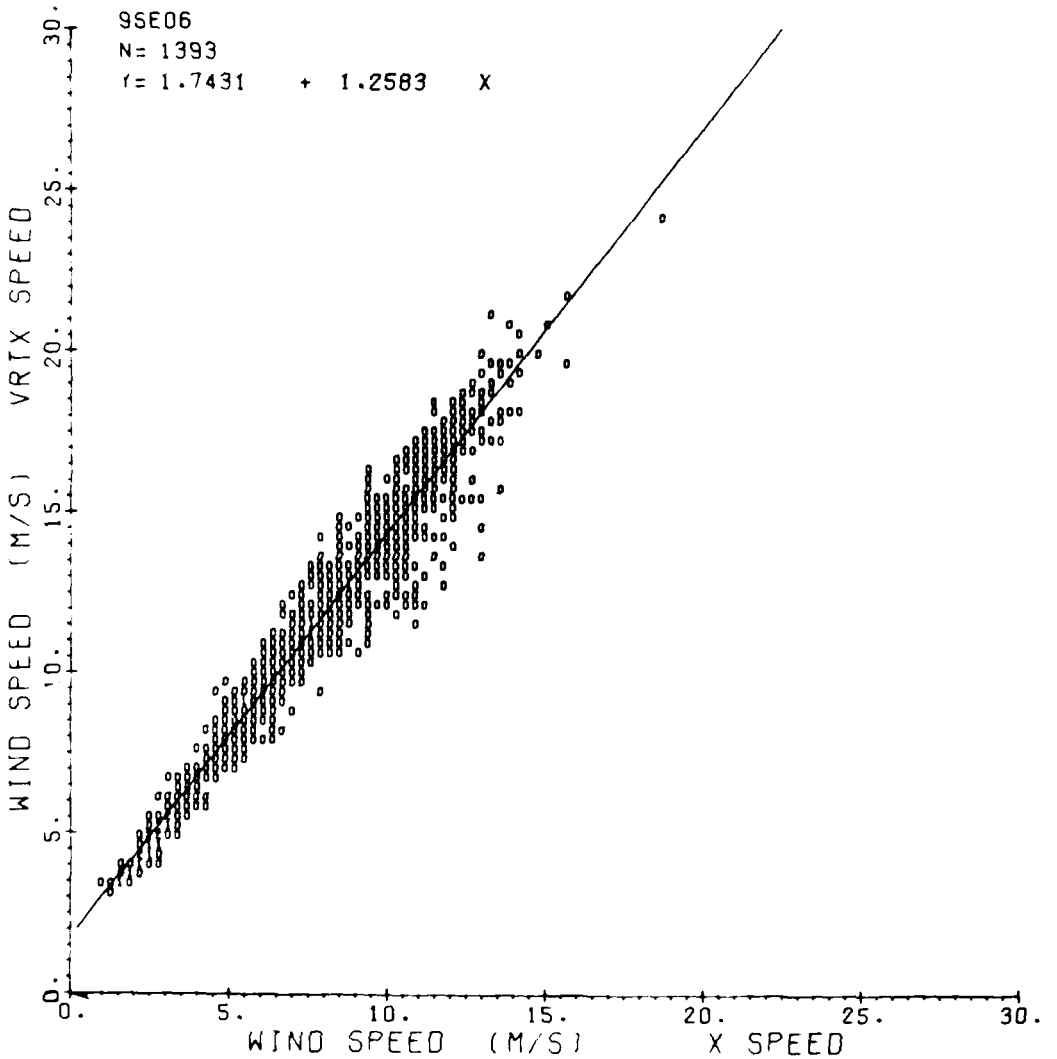

Figure B-2. Comparison between Vortex and Climatronics (X) wind speeds.

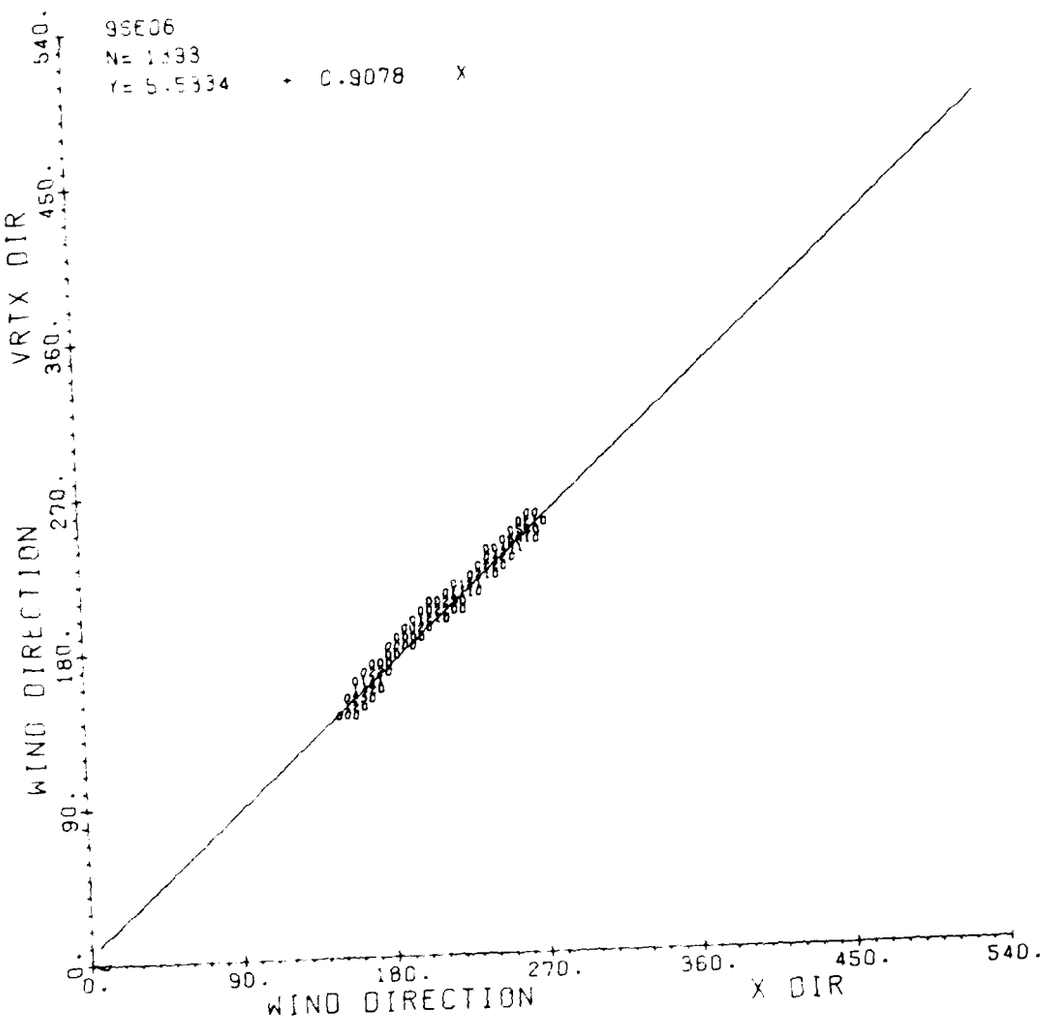

Figure B-1. Comparison between Vortex and Climatronics (X) wind directions.

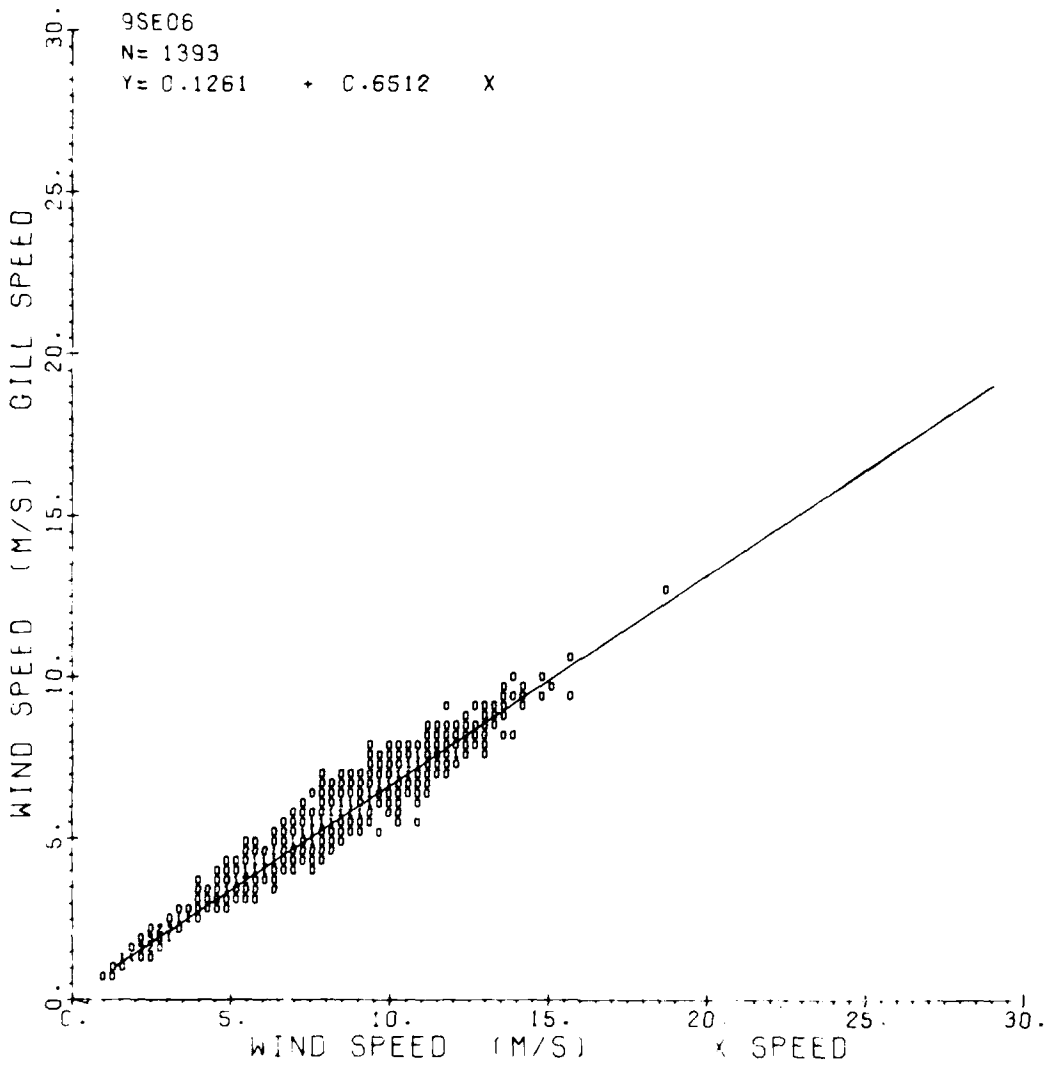

Figure B-1. Comparison between Gill and Climatronics (X) wind speeds.

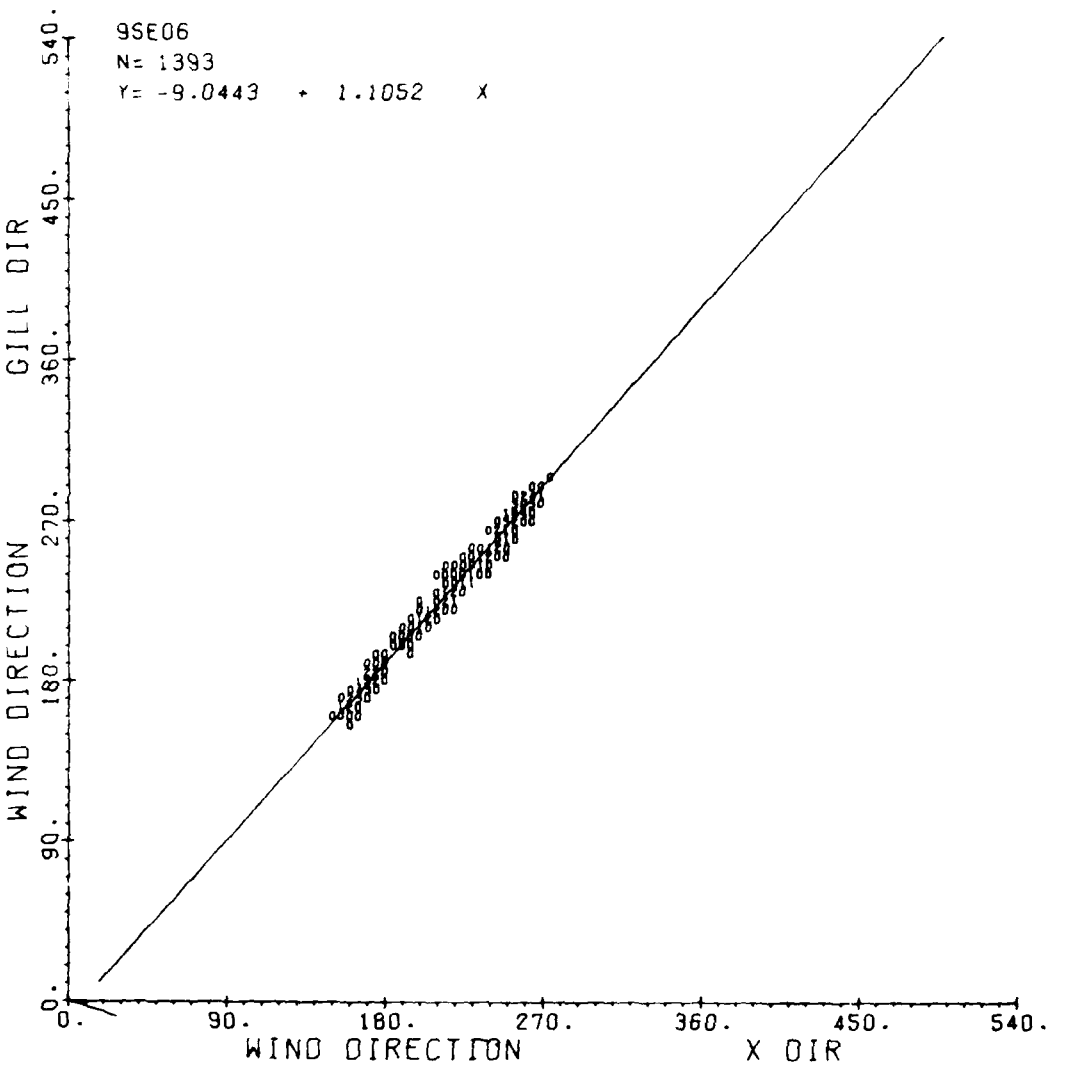

Figure B-5. Comparison between Gill and Climatronics (X) wind directions.

WEATHER SYMBOLS

	T	Thunderstorm
	T+	Severe Thunderstorm
	A	Hail
	IC	Ice Crystals
	IP(W)	Ice Pellets(Showers)
●	L	Drizzle
●	R	Rain
	RW	Rain Showers
●	S	Snow
	SG	Snow Grains
	SP	Snow Pellets
	SW	Snow Showers
●	ZL	Freezing Drizzle
●	ZR	Freezing Rain

OBSTRUCTIONS TO VISION

	BD	Blowing Dust
●	BN	Blowing Sand
●	BS	Blowing Snow
	BY	Blowing Spray
●	K	Smoke
●	H	Haze
	D	Dust
●	F	Fog
●	GF	Ground Fog
●	IF	Ice Fog

PRECIPITATION INTENSITY SYMBOLS

	--	Very light
●	-	Light
●	+	Heavy

● Absence of symbol indicates moderate except for A and IC

Figure B-6. Circles indicate elements specified by decision-tree program.

C. McIDAS HARDWARE AND SUPPORT TO RESEARCH PROJECTS

I. INTRODUCTION

SASC's objective is to improve the output of the AFGL/Meteorology Division McIDAS Facility and to operate it in support of meteorological research. As an interactive system McIDAS combines its resident programs and processing speed with the skill and ingenuity of the user, to facilitate handling large masses of data. It acquires, processes, and analyzes satellite and conventional weather data. Visible and infrared satellite data are received from two geosynchronous satellites operated by NOAA/NESS. Conventional data (surface and upper air reports) arrive via high speed FAA data line.

II. McIDAS HARDWARE ENHANCEMENT

McIDAS consists of a real-time data acquisition subsystem, Harris 6024/5 computer with 65K memory (24-bit word length), 80 megabyte digital disk drive, four additional disk drives each with 10 megabyte capacity, line printer, card reader, two tape transports for 9-track 800 BPI magnetic tapes, IVC video disk recorder with a total capacity of 500 frames, and two CRT keyboard consoles for the system operators.

A major system improvement was the installation of the 80 megabyte digital disk, which not only provides additional storage capacity but can access data at a much faster rate than the other four disks with combined megabyte capability. When both terminals are used simultaneously, the older information retrieval [illegible] with [illegible] units, plotter output [illegible].

[illegible] (Wm^{-2} sr^{-1}). [illegible]

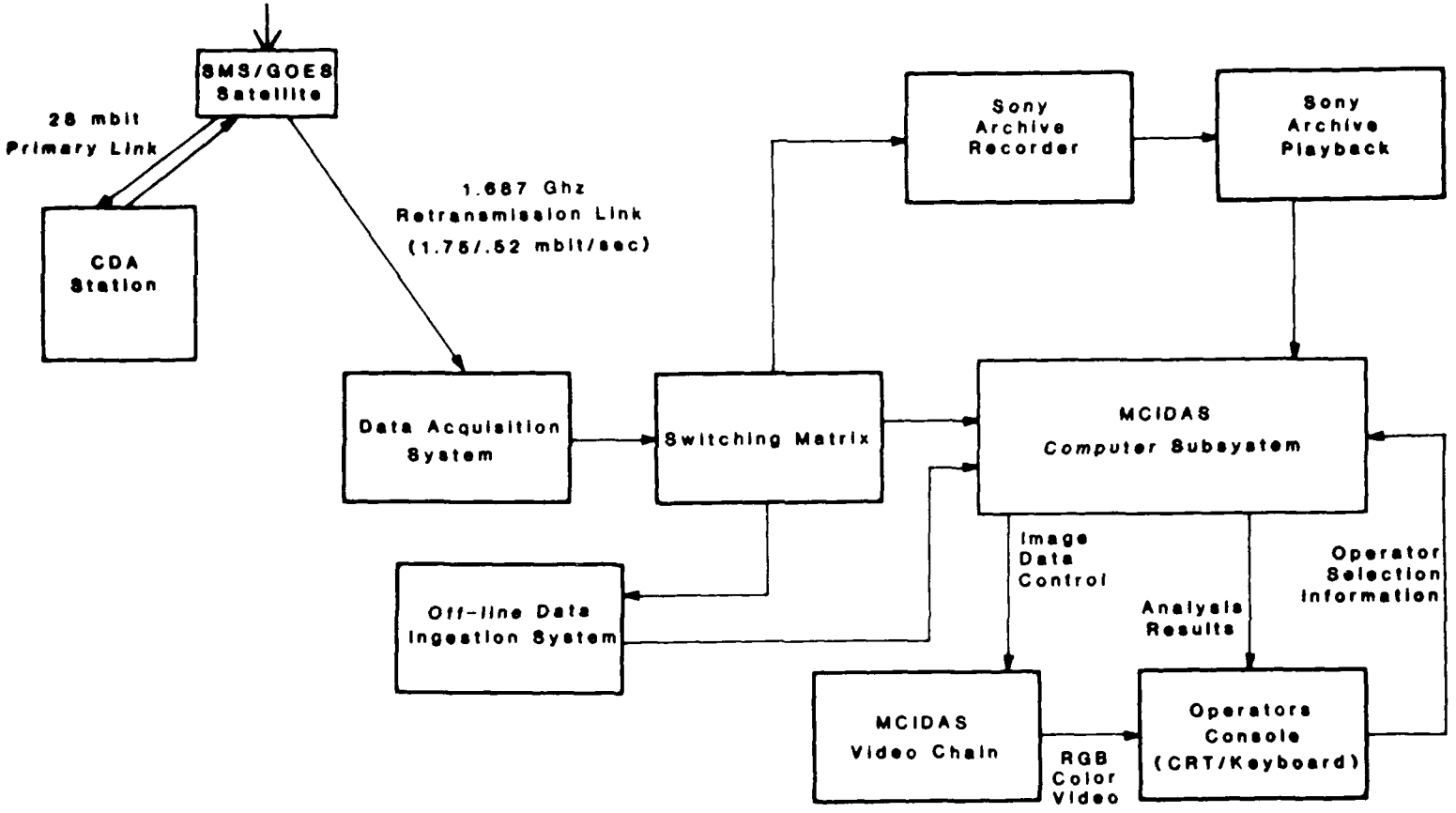

Figure C-1. McIDAS functional block diagram.

as transmitted every half-hour from the satellite. Sony archive recorder components include a modified VO-2850A video cassette recorder, a motor drive amplifier to run the recorder at 500 rpm, and the encoding electronics to format GOES/SMS data for recording on tape. Player components are a modified VP-1200 video cassette player, a motor drive amplifier to run the player scanner at 500 rpm, an Aydin Monitor Model 350 bit synchronizer, and decoding electronics to reconstruct GOES/SMS data as well as to provide search information and remote control capability. The University of Wisconsin Space Science and Engineering Center assembled the system, to which a switching matrix and byte mangler were added to integrate fully the archive units with McIDAS. Two archive systems were installed; one on-line, the other as a spare in anticipation of simultaneous recording from two satellites.

McIDAS data lines were removed and replaced with a full duplex dataphone system. The Dataset 212A is capable of transmitting and receiving data at a rate of 1,200 BPS. System compatibility with the University of Wisconsin installation now makes exchange of software technically feasible.

Modifications were made in the cursor control electronics in an effort to stabilize the cursor position generated by the joysticks. Redesign employed a +18 volt and -8 volt isolated power supply instead of the +18 volts supplied from the system. The isolated power supply, along with resistors on both ends of the joysticks, decreased cursor fluctuations.

Acquisition of a Tektronix video monitor and associated camera unit has given McIDAS the ability to produce hard-copy prints of imagery stored on the video disk. This eliminates the necessity of using an entire tape in order to save one or two images. In addition, prints can be made of conventional data such as surface and upper air plots and analyses. Figures referenced below are prints taken with the monitor camera.

III. McIDAS SUPPORT TO RESEARCH PROJECTS

McIDAS supported a series of ABRES (Advanced Ballistic Re-entry System) missions conducted at the Kwajalein Missile Range (KMR). Missions were weather-dependent, categorized as heavy weather, moderate weather, or clear air, according to the conditions desired for re-entry.

Because of the isolation of Kwajalein and the absence of surrounding surface stations, local weather observers depended heavily on radar and ship/aircraft reports when making forecasts. Prior to mission time, McIDAS provided KMR forecasters with a single image showing cloud top temperatures, a cross-correlation of two or more images that yielded wind vectors, and loops of several images that depicted cloud growth and decay.

Another valuable input to ABRES was the Environmental Severity Index (ESI), which was a measure of particulate matter at various levels in the atmosphere. The measurement indicated the potentially erosive effects of such matter on a re-entry vehicle. On several occasions McIDAS was instrumental in determining whether a mission count down was to continue to launch or not.

The Large Scale Cloud System Program, a continuing AFGL effort to obtain better definition of the microphysics of large winter storms, sampled extensive homogeneous cloud masses as they progressed from west to east over North America. Aircraft data relating to particle size, type, number, and liquid water content were collected at various atmospheric levels. McIDAS satellite imagery loops showing cloud motion and cloud top temperatures enabled the ground support group to identify the most desirable sampling locations to the inflight crew. Because of the high cost of flight operations it was important for the aircraft to reach the best location as quickly as possible. McIDAS provided conventional surface observation plots and analyses of wind vectors, pressure fields, streamlines, dew point temperatures, precipitation amounts, current weather, visibility, and cloud cover conditions (see Figs. C-2, C-3, C-4, and C-8). Also, upper

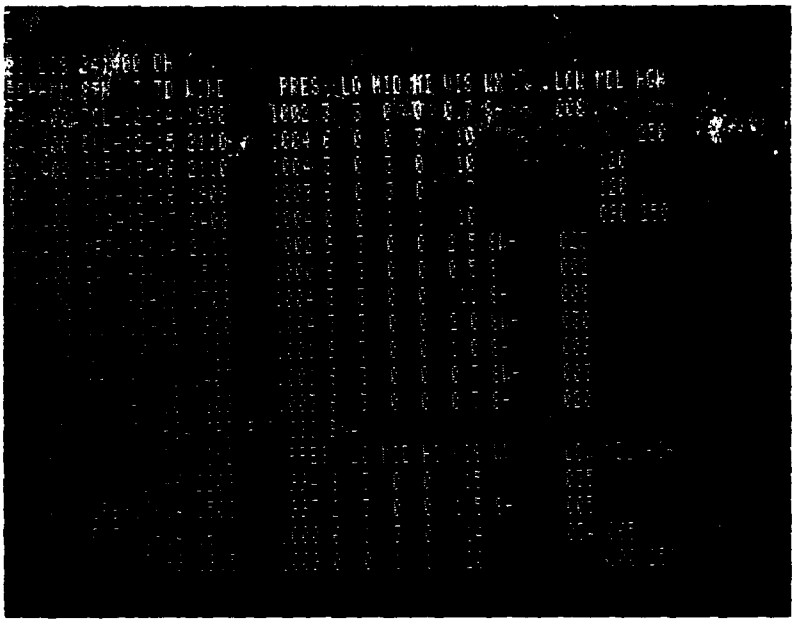

Figure C-2a. All Ohio surface station reports; (lower) list of individually selected stations.

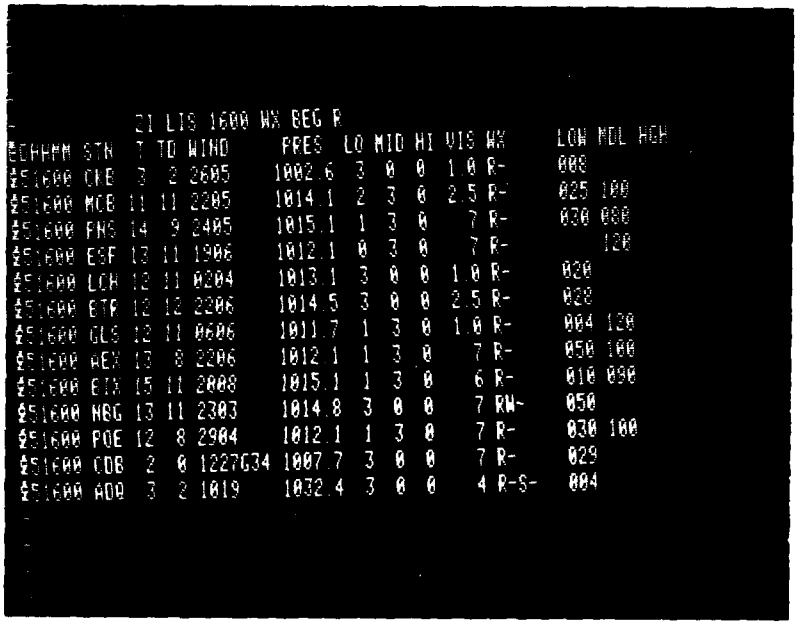

Figure C-2b. All surface stations reporting rain.

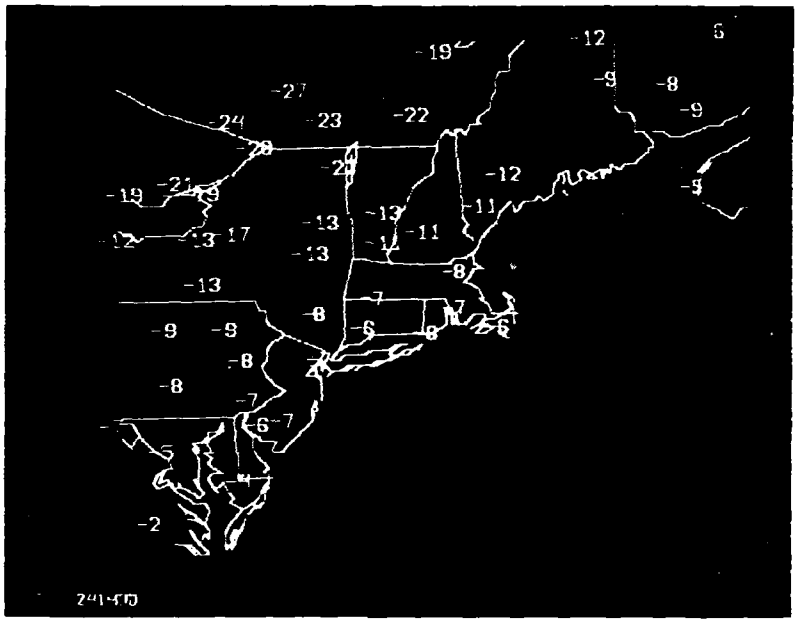

Figure C-3a. Surface temperature plot centered on Massachusetts.

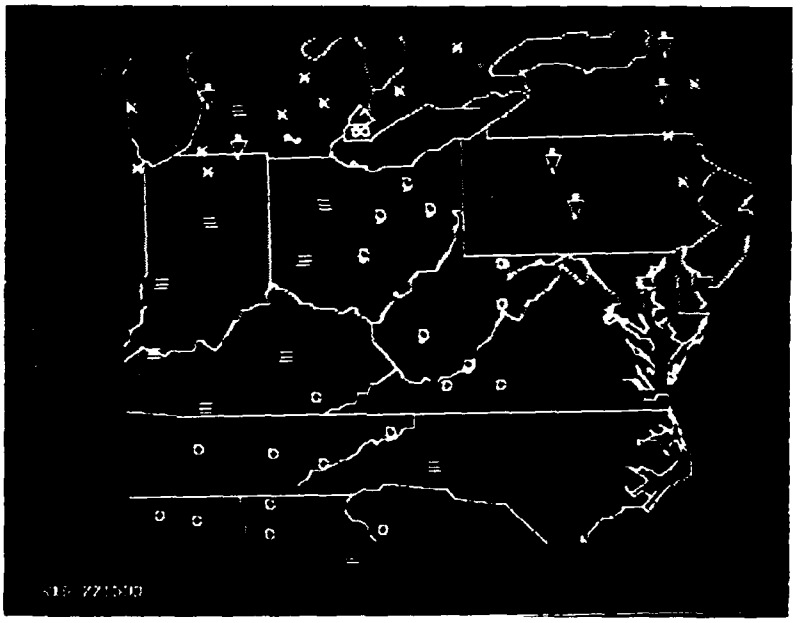

Figure C-3b. Surface weather symbols centered on West Virginia.

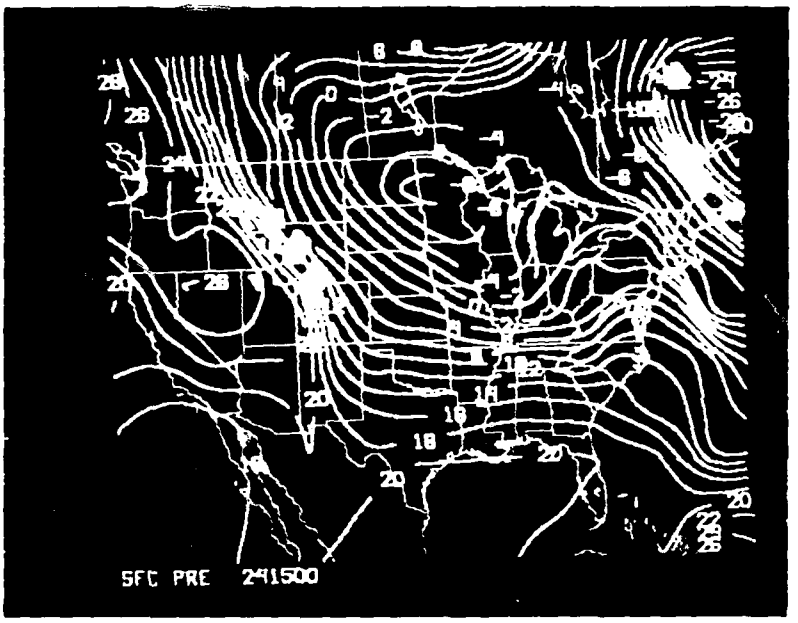

Figure C-4a. Surface pressure analysis for the U.S. The 20 isobar = 1,020 mb; -4 isobar = 996 mb.

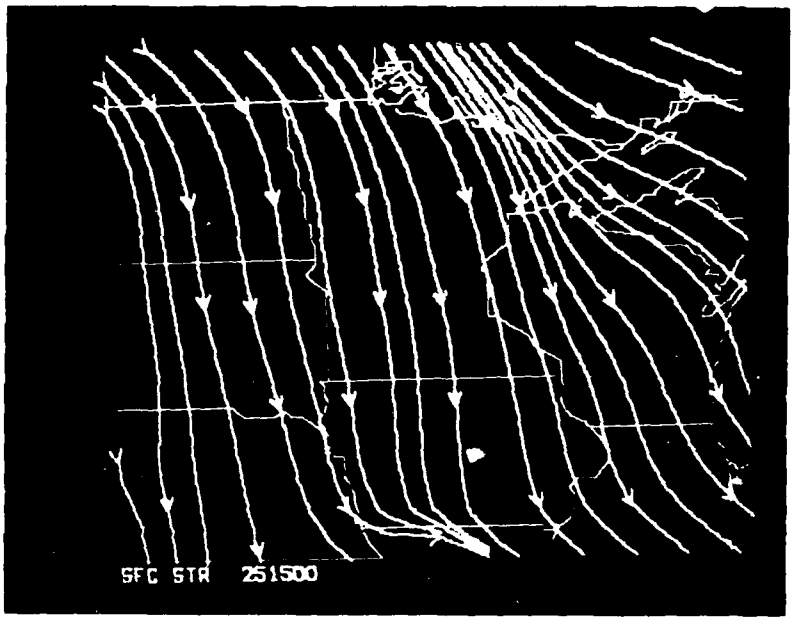

Figure C-4b. Surface analysis of wind flow (streamlines) centered on Minnesota.

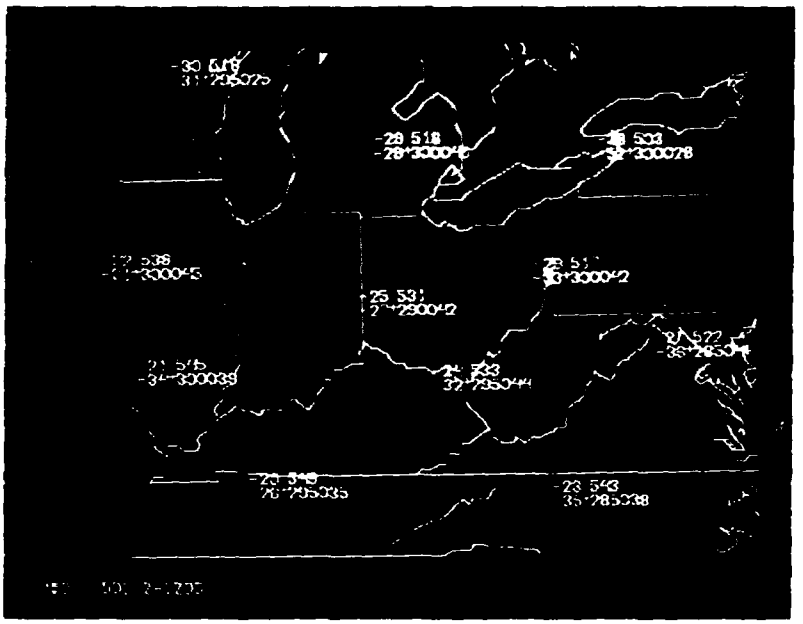

Figure C-5a. 500 mb station model plot centered over Ohio.

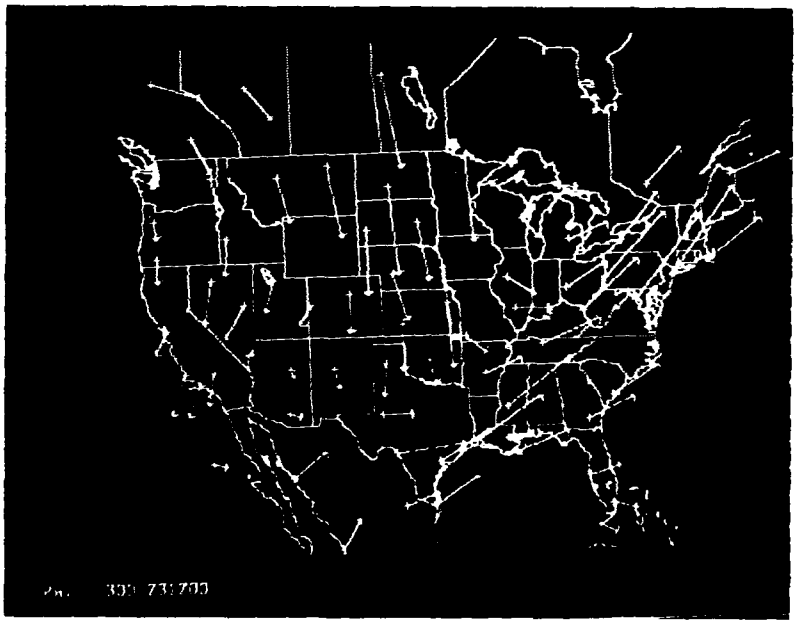

Figure C-5b. 300 mb wind vectors for the United States.

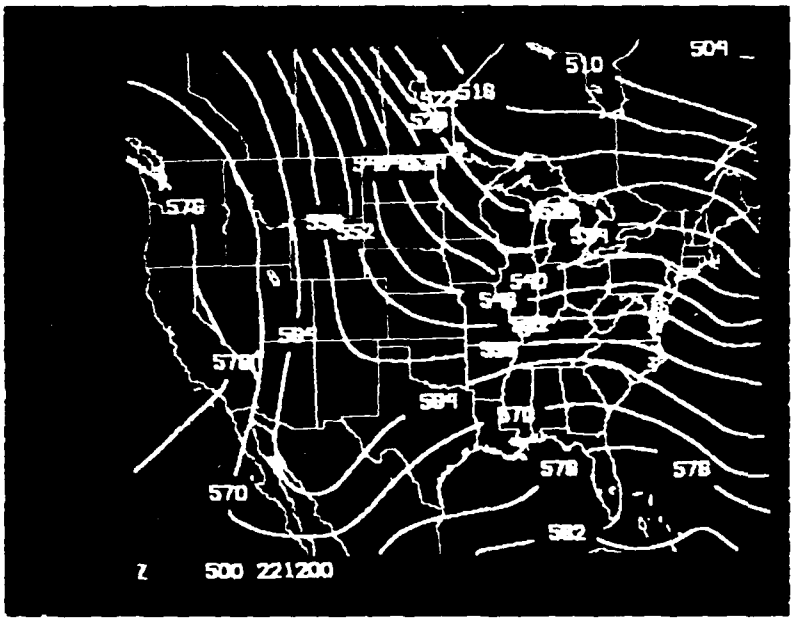

Figure C-6a. 500 mb height analysis for the United States.

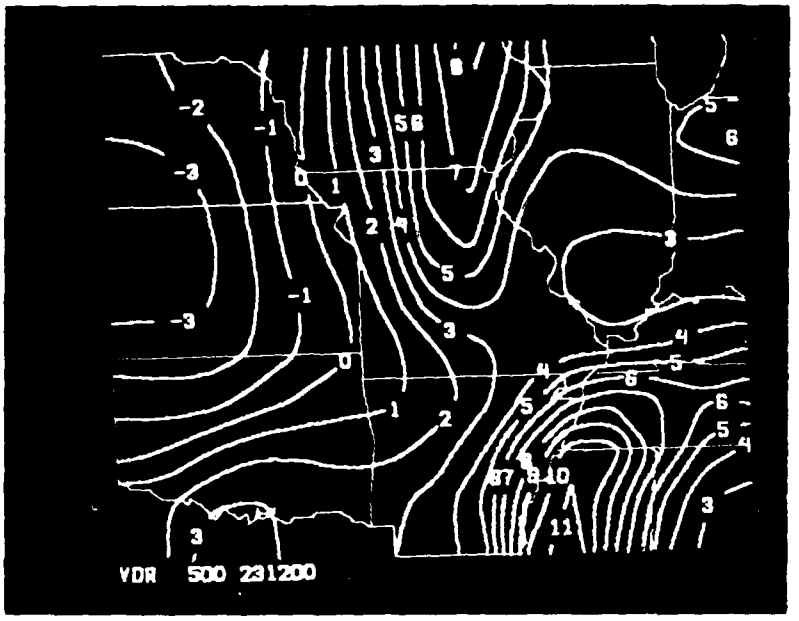

Figure C-6b. 300 mb vorticity analysis centered on Missouri.

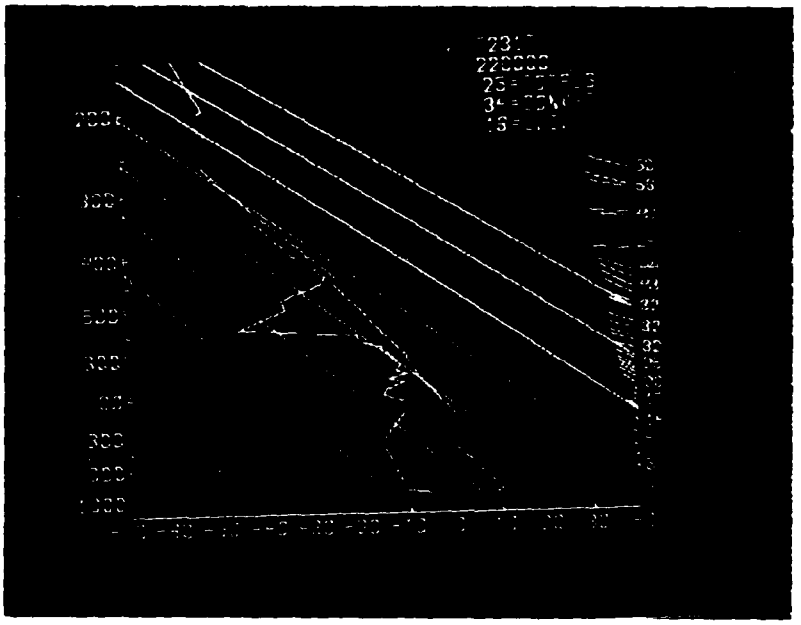

Figure C-7a. Stuve diagram; top at 150 mb.

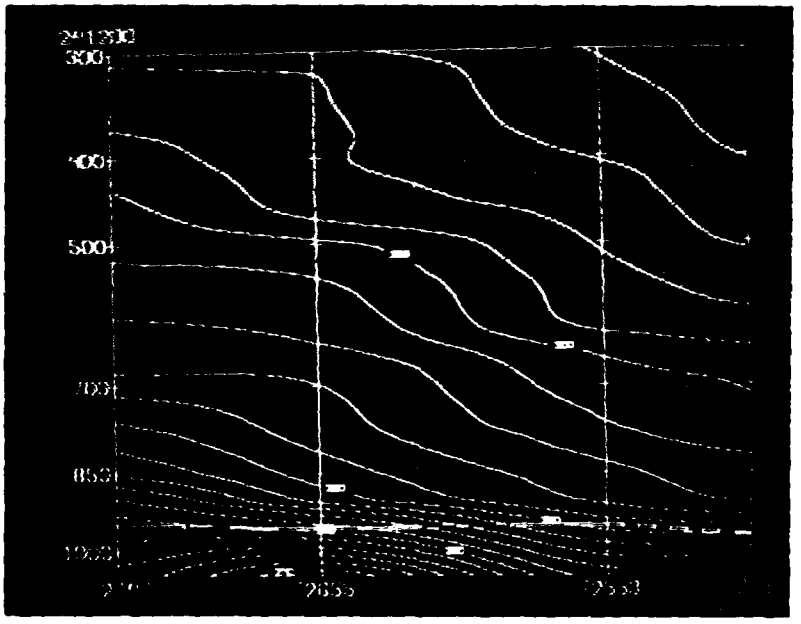

Figure C-7b. Vertical cross-section of potential temperature; top at 300 mb.

air height analyses, vorticity analyses, and radiosonde (Stuve) and cross-section plots (see Figs. C-5, C-6, C-7) helped determine suitable sampling altitudes. Data were then archived on tape and hard-copy printouts for later documentation of the synoptic situation.

Another on-going study requiring McIDAS support was the Mesoscale Forecasting Program. It was concerned with developing short range forecast techniques using sequences of GOES/SMS imagery. A microprocessor-controlled tape drive known as ODIS (Off-line Data Ingestion System; see Fig. C-1) collected one-mile visible, four-mile infrared images centered over eastern Pennsylvania, at hourly intervals from 1400Z to 2100Z. Data were collected at half-hourly intervals if the study area contained particularly interesting or severe weather. Collected data were then saved on magnetic tape, three days' data per tape. The data were analyzed on the AFGL central computer to yield motion vectors, brightness, and IR temperatures which were converted into weather parameters for the forecast procedures.

The AFGL Icing Program was designed to observe and measure accumulation of ice on an aircraft. Five flights were conducted with an instrumented C-130 aircraft, which sampled over any one of 12 radiosonde stations within a 300-mile radius of Wright-Patterson AFB, Ohio. Sequences of visible and IR imagery were provided by McIDAS to determine if suitable icing conditions existed within the study area. Other data included hourly FAA surface observations of current weather (see Fig. C-8), temperature, dew point temperature, pressure, wind speed and direction, cloud cover and ceiling, 6-hour precipitation total, streamlines (see Figs. C-2, C-3, C-4), upper air height analyses, radionsonde and cross-section plots (see Figs. C-5, C-6, C-7). Again, preflight and in-flight data were archived on tape and printouts for later inspection at report time.

IV. DATA NAVIGATION IMPROVEMENT

When working with satellite data it is important to know precisely the latitude and longitude of any given point within the field of view. The situation is exacerbated if the imagery contains an expanse of ocean or cloud-obscured land. To insure maximum location accuracy of satellite data, a navigation program was developed at the University of Wisconsin Space Science and Engineering Center. That program relates a simplified orbital model in McIDAS to the scan line and element of the satellite. Orbital data used in the navigation process are computed by NOAA from a complex model taking into account several celestial bodies. Since the McIDAS orbital model is only a two-body system it frequently requires adjustment when a manuever (re-orientation) occurs or when an orbit decays.

Real-time data used in the navigation procedure (see Fig. C-9) are 0.5 mi resolution images, enlarged on the TV screen by a factor of four. The landmark is generally a prominent point along a coastline with a distinct land/sea interface. After five to seven images have been ingested, the landmark common to all is defined; that is, the latitude and longitude of the particular point are called up from a locate file and entered into the system. An acetate overlay map is placed over the TV screen, with a cross-hair centered on the exact point. Once image and overlay are aligned, a digital cursor on the TV screen is matched to the cross-hair and the satellite scan line and element are measured. Values from each image are compared with the line and element numbers derived from the McIDAS model. Differences between the two sets are known as the residuals. If the residuals are small (less than ± 2.50, 0 being perfect) it is considered a good orbit. Large residuals indicate that adjustment of one or more of the NOAA orbital parameters is necessary. Extremely large residuals indicate that a new orbit may be necessary. In 1979 SASC initiated a project to develop a logical methodology for adjusting orbital parameters.

As a brief example, Fig. C-10 is a navigation print-

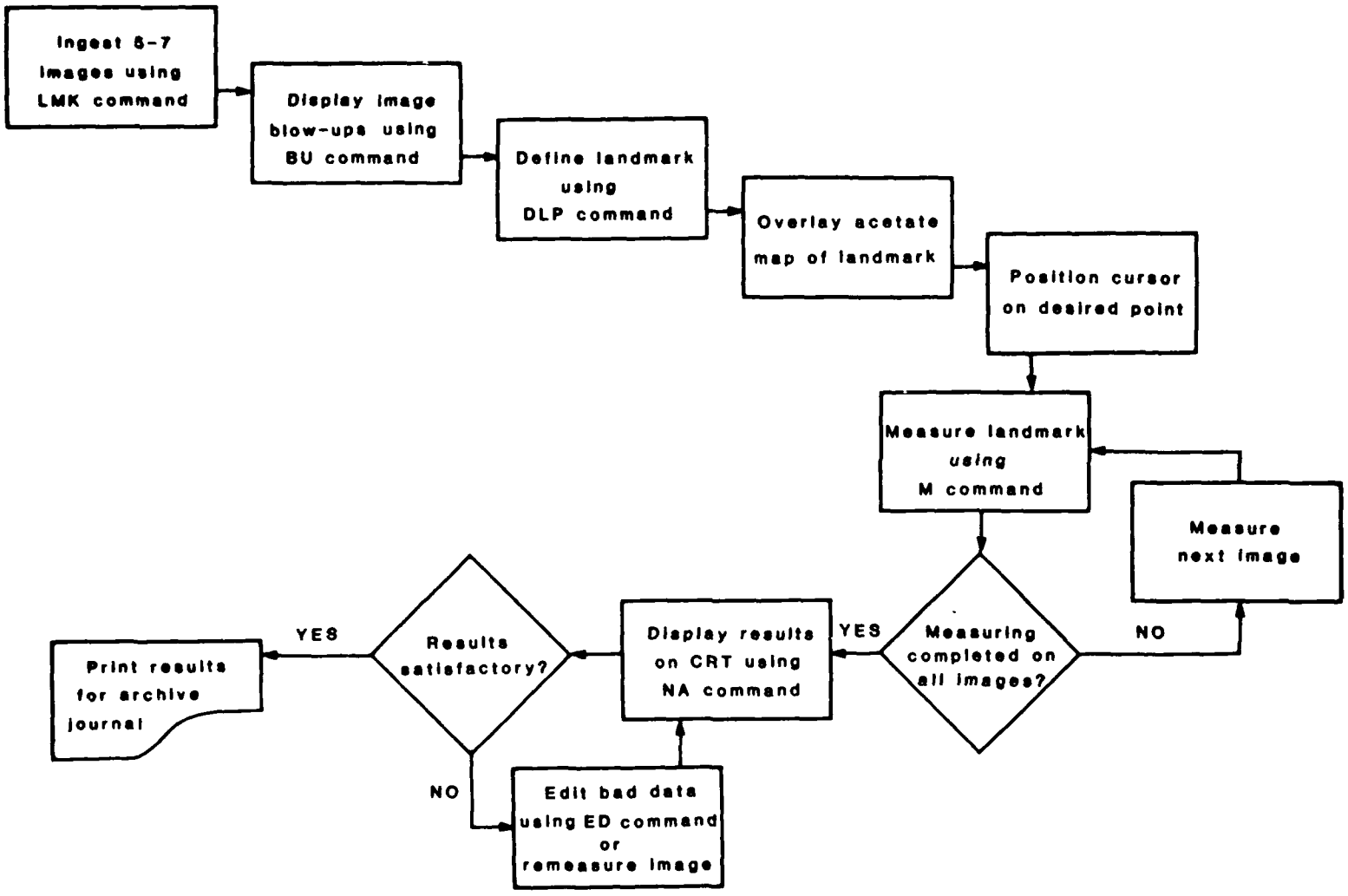

Figure C-9. Navigation procedure.

```
   ***    A F G L   M C I D A S          ***      PROGRAM:  SYSNAV

NAVIGATION FOR  1879332      (28 NOV 1979)
LANDMARKS. . .
LM     1.   140000          0      6423      9128    103910   -641600
LM     2.   143000          0      6426      9126    103910   -641600
LM     3.   150000          0      6428      9122    103910   -641600
LM     4.   153000          0      6429      9121    103910   -641600
LM     5.   160000          0      6430      9119    103910   -641600
LM     6.   163000          0      6432      9118    103910   -641600
BETAS. . .
BT     1.   140000          1       180    140147        93 -5400578
BT     2.   140000          2       853    140829        74 -5429869
BT     3.   143000          1       360    143334        90 -5539595
BT     4.   143000          2       849    143826        85 -5560879
BT     5.   150000          1         4    150001        85 -5655283
BT     6.   150000          2       852    150828        74 -5692235
BT     7.   153000          1       184    153149        72  5739208
BT     8.   153000          2       849    153826        76  5710267
BT     9.   160000          1       178    160146        24  5608257
BT    10.   160000          2       850    160827        46  5579013
BT    11.   163000          1       172    163142        76  5477317
BT    12.   163000          2       852    163828        76  5447727
FRAME GEOMETRY
F       SMS  200000  801821  182230    15288
CAMERA GEOMETRY
C       SMS   -3930       0       0
BETA CONSTANTS
BC      SMS -114033 1390000
SPIN RATE
S  1879332  596970
ORBIT
O   791110  200000 4216762     663     185   69042  113998   91557
PRECESION
P  1879332       0       0
SKEW
D  1879332       0
ATTITUDE
A  1879332  894732 3504535    7285(  6) GNORM=   .375795E-10  VALUE
GAMMA SHIFTS
IAJUST=   -114033     IAJTIM=    140000
G    1. 1879332  140000    12093     -103 (    1 )
G    2. 1879332  143000    12709     -145 (    1 )
G    3. 1879332  150000    12219     -111 (    1 )
G    4. 1879332  153000    10627       -7 (    1 )
G    5. 1879332  160000    10872      -24 (    1 )
G    6. 1879332  163000    10345        8 (    1 )
RESIDUALS                              LINE    ELEMENT
R    1. 1879332  140000       0      -.88      -.04     1020 -751943    721
R    2. 1879332  143000       0      -.18      -.61      941 -751909    558
R    3. 1879332  150000       0      -.19     -3.21      852 -751836    429
R    4. 1879332  153000       0      -.86     -2.64      754 -751803    255
R    5. 1879332  160000       0     -1.17     -3.29      648 -751733    119
R    6. 1879332  163000       0      -.09     -2.85      535 -751705    -19
```

Figure C-10. Navigation printout from November 28, 1979.

out from November 28, 1979. From the residuals it is apparent that the orbit for that day was discrepant. Minor adjustment was sufficient to bring the residuals within acceptable range. One orbital parameter whose increase or decrease greatly affects the residuals is the semi-major axis, which is defined as one-half the greater axis of the ellipse of motion. The semi-major axis in Fig. C-10 is 42,167.62 km. Reducing it by 3 km to 42,164.62 (see Fig. C-11) reduces the residuals to acceptable values. Thus, given any point within the landmark images, its location would be less than one nautical mile in error. Although adjusting the orbital parameters is not done daily, the imperfect satellite orbit requires that navigation be done daily. A good orbit should last approximately two weeks before the residuals become excessive.

Other orbital elements - eccentricity, inclination, mean anomaly, argument of the perigee, and right ascension - remain to be investigated.

```
***     A F G L   M C I D A S                          PROGRAM:  SYSNAV

NAVIGATION FOR  1879332      (28 NOV 1979)
LANDMARKS. . .
LM     1.   140000          0      6423      9128    103910   -641600
LM     2.   143000          0      6426      9126    103910   -641600
LM     3.   150000          0      6428      9122    103910   -641600
LM     4.   153000          0      6429      9121    103910   -641600
LM     5.   160000          0      6430      9119    103910   -641600
LM     6.   163000          0      6432      9118    103910   -641600
BETAS. . .
BT     1.   140000          1       180    140147        93 -5400578
BT     2.   140000          2       853    140829        74 -5429869
BT     3.   143000          1       360    143334        90 -5539595
BT     4.   143000          2       849    143826        85 -5560879
BT     5.   150000          1         4    150001        85 -5655283
BT     6.   150000          2       852    150828        74 -5692235
BT     7.   153000          1       184    153149        72  5739208
BT     8.   153000          2       849    153826        76  5710267
BT     9.   160000          1       178    160146        24  5608257
BT    10.   160000          2       850    160827        46  5579013
BT    11.   163000          1       172    163142        76  5477317
BT    12.   163000          2       852    163828        76  5447727
FRAME GEOMETRY
F       SMS  200000  801821  182230   15288
CAMERA GEOMETRY
C       SMS   -3930       0       0
BETA CONSTANTS
BC      SMS -114033 1390000
SPIN RATE
S  1879332  596970
ORBIT
O   791110  200000 4216462     663     185   69042  113998   91557
PRECESION
P  1879332       0       0
SKEW
D  1879332       0
ATTITUDE
A  1879332  894732 3503856    7285(  6) GNORM=    .405624E-10  VALUE
GAMMA SHIFTS
IAJUST=   -180612    IAJTIM=    140000
G   1. 1879332  140000      484       35 (    1 )
G   2. 1879332  143000     1145      -11 (    1 )
G   3. 1879332  150000      699       20 (    1 )
G   4. 1879332  153000     -844      121 (    1 )
G   5. 1879332  160000     -553      101 (    1 )
G   6. 1879332  163000    -1027      130 (    1 )
RESIDUALS                          LINE     ELEMENT
R   1. 1879332  140000        0     -.75       .04     1017 -743840    712
R   2. 1879332  143000        0     -.10       .14      937 -743803    549
R   3. 1879332  150000        0     -.12     -1.69      847 -743728    419
R   4. 1879332  153000        0     -.81      -.35      748 -743652    245
R   5. 1879332  160000        0    -1.11      -.28      641 -743619    108
R   6. 1879332  163000        0     -.02       .91      528 -743549    -29
```

Figure C-11. Reduction of semi-major axis by 5 km.

D. McIDAS SYSTEMS AND APPLICATIONS SOFTWARE

I. INTRODUCTION

McIDAS software improvement involved two types of activities - modifying existing programs and adding new ones. The first included correcting logic faults and key-punching errors, increasing utility of individual programs by adding new functions, and adjusting programs to accommodate extensive changes in the hardware system. Certain new programs were supplied by the University of Wisconsin and adapted for the AFGL McIDAS, while others were written by SASC to meet specific needs of AFGL and SASC scientists.

II. MODIFICATIONS

By early 1979 all system software and most applications software originally provided by the University of Wisconsin had been implemented. However, one category of programs called NOWCASTING still contained logic errors. Since these programs, designed to analyze and display conventional weather data, are used routinely for monitoring current weather, such faults quickly became apparent and were corrected. Additional functions were included to expedite location and identification of individual surface and radiosonde stations, and a plot file capability was added to those programs written for WRRRM (Write Random Read Raster Memory) display only. This modification makes it possible to write into the display file and transfer the finished product to a TV frame.

The modifications required to make the programs written for the University of Wisconsin McIDAS compatible with the AFGL system were due primarily to configurational differences between the two facilities. One major difference, for example, involved the form in which support software was stored on disk. Most AFGL support routines

existed as individual relocatable modules, whereas the University of Wisconsin had gathered them into specialized libraries. Not only does the latter procedure reduce the amount of disk storage required but also simplifies the job control stream of most applications programs. AFGL software was therefore reorganized to incorporate this improved structure.

The addition of the Sony video cassette archive necessitated adaptation of the real-time satellite ingest program and support routines to permit ingestion of imagery from the archive playback unit. Two test programs provided by the University of Wisconsin for sampling the quality of recorded imagery were also implemented.

Increase in mass storage afforded by the addition of an 80 megabyte disk made feasible an increase from 16 to 24 in digital areas available to each user terminal for storage of satellite imagery. This increase required creation of new data files and adaptation of every applications program, system routine, and library module which must have access to them.

III. NEW PROGRAMS

Additional storage space also became available for new programs. The Area Statistics software package, from the University of Wisconsin, is a collection of programs and data files designed to select portions of satellite images and perform statistical analyses on the digital data they represent. Although these programs are still in the developmental stage, functions which are available include calculation of brightness distributions in histogram form, surface areas, and area sums lying between, above, below, or at specific brightness levels.

The largest addition to McIDAS software was a collection of relocatables, data files, and a main driver program, designated the Mesoscale Forecasting Facility (MFF). Motivation for this major programming effort was the Air Force desire to make the many valuable McIDAS forecasting aids available to all AFGL Mesoscale Forecasting Branch

meteorologists and to encourage regular exercise of short-range prediction skills.

IV. MESOSCALE FORECASTING FACILITY (MFF)

With only minimal knowledge of McIDAS operating procedures, a forecaster using MFF can access most of the NOWCASTING programs and many satellite imagery request and display functions, formulate a forecast, enter his predictions into a personalized data file, verify the forecast at a later time, and evaluate his performance by reviewing his past forecasts and accumulated skill scores.

MFF is a menu-driven program; that is, instruction pages present a series of multiple-choice questions. Answers provided by the forecaster are used to build normal McIDAS commands performing a variety of functions which assist in formulating, inputting, and verifying short-range (1-6 hr) forecasts.

The MFF program consists of four major components - chief forecaster, operational forecaster, interrogation, and verification modules. The chief forecaster module enables the responsible scientist to select the station for which the day's forecasts are to be made and the parameters (predictands) whose values are to be forecast. He also leads a brief discussion of current weather conditions. Operational forecasters participate in the weather discussion and, using the operational forecaster module, formulate forecasts in compliance with the specifications set by the chief. The interrogation module permits the operator to review his performance to date by listing past forecasts and accumulated skill scores. The verification module compares the predictions of each forecaster with the actual station reports and computes individual skill scores.

A. CHIEF FORECASTER MODULE

The primary component of MFF is the module for the chief forecaster. After careful examination of the most recent weather data, including conventional surface and upper

air reports and real-time satellite imagery, the chief forecaster chooses a region exhibiting interesting meteorological features and provides a selection of challenging forecast parameters.

Three media are available for conventional data representation. The most flexible method utilizes the video graphics display capabilities of McIDAS. Plots and contoured analyses of surface and upper air data are produced in three colors on a TV monitor. Values of any reported parameters and some additional derived parameters (Tabs. D-1 and D-2) may be plotted over U.S. or regional base maps. Fig. C-3a is an example of a surface temperature plot over New England. In addition to digital data, special symbols are available for representation of sky cover and weather (Fig. C-3b). Wind speed and direction can be displayed in three forms: digitally as in the station model plot depicted in Fig. C-5a, vectorially as in Fig. C-5b, and as standard meteorological flags. Those parameters which exist as continuous or nearly continuous fields (Tabs. D-3 and D-4) can be interpolated to grid point values and objectively contoured. Figs. C-4 and C-6 show examples of surface and upper air analyses performed in this manner and displayed by McIDAS. Two additional types of analyses are available for radiosonde reports. Individual station reports in the form of Stuve thermodynamic diagrams (Fig. C-7a) are useful in estimating stability. Groups of four to six reports organized in spatial or temporal series, analyzed as vertical cross-sections or time sections, provide a detailed view of the distribution of thermal, moisture, and velocity fields in the atmosphere (Fig. C-7b).

The time required for McIDAS to generate any of these types of displays is normally less than two minutes, depending on the extent to which the system is involved in other activities concurrently. As leader of the weather discussion, the chief may find that this time delay severely limits the number of parameters he is able to present. His module therefore provides the option to save the specifications for up to five commands generated while preparing his presentation. A minor amount of time is

Table D-1. Parameters Available for Surface Data Plots

Temperature	*Wind flags
Dew point temperature	Visibility
Pressure	Wind gusts
Wind direction and speed	Precipitation
Low cloud cover	Low cloud height
Middle cloud cover	Middle cloud height
High cloud cover	High cloud height
Current weather	*Ceiling height
*Current weather symbols	**Potential temperature
	**Equivalent potential temperature

*Not available on line printer plots
**Available on line printer only

Table D-2. Parameters Available for Upper Air Data Plots

Station identifiers
Temperature
Dew point temperature
Wind direction and speed
Heights
*Wind flags
*Wind vectors
Plot all parameters in station model format

*Not available on line printer plots

Table D-3. Parameters Available for Surface Data Contouring

Temperature	Dew point advection
Dew point temperature	Mixing ratio advection
Pressure	Streamlines
Potential temperature	Ceiling height
Equivalent potential temperature	Stretching deformation
	Shear deformation
Mixing ratio	Dew point divergence
Wind speed	Mixing ratio divergence
Total cloud cover	Visibility
Divergence	Low cloud cover
Vorticity	Middle cloud cover
Temperature advection	High cloud cover

Table D-4. Parameters Available for Upper Air Data Contouring

Temperature	Vorticity
Dew point temperature	Temperature advection
Heights	Dew point advection
Potential temperature	Mixing ratio advection
Equivalent potential temperature	Streamlines
	Stretching deformation
Mixing ratio	Shear deformation
Wind speed	Dew point divergence
Total cloud amount	Mixing ratio divergence
Divergence	

still required to retrieve and analyze the data and draw the display on the TV screen. If more than five charts are desired, or if the time allotted for producing each one must be further reduced, a second display medium is available. Any of the above types of displays may be written into a plot display file and transferred to the analog disk where they are preserved for future use. Images produced in this manner forfeit the advantage of color.

The third display medium provides a means of producing hard copies of most of the charts described. Line printer output is requested in lieu of TV display. Surface and upper air data plots are printed over a U.S. base map. Fig. D-1 shows a line printer plot of current weather. (Special weather symbols seen in Fig. C-3b are not available through this device.) The temperature plot in Fig. D-2 illustrates the approximate coverage of surface data. Upper air coverage is shown in Fig. D-3 by a plot of the five-digit identifiers of all reporting radiosonde stations. Contouring of data is simulated on line printer output by alternate shading between contours. Examples of surface analyses of this type are shown covering the U.S. in Fig. D-4 and on a regional scale in Fig. D-5. Upper air charts analyzed in this fashion are also available. Examples of 500 mb heights and vorticity are given in Figs. D-6 and D-7 respectively. While soundings, cross-sections, and time sections cannot be provided in analyzed form by the line

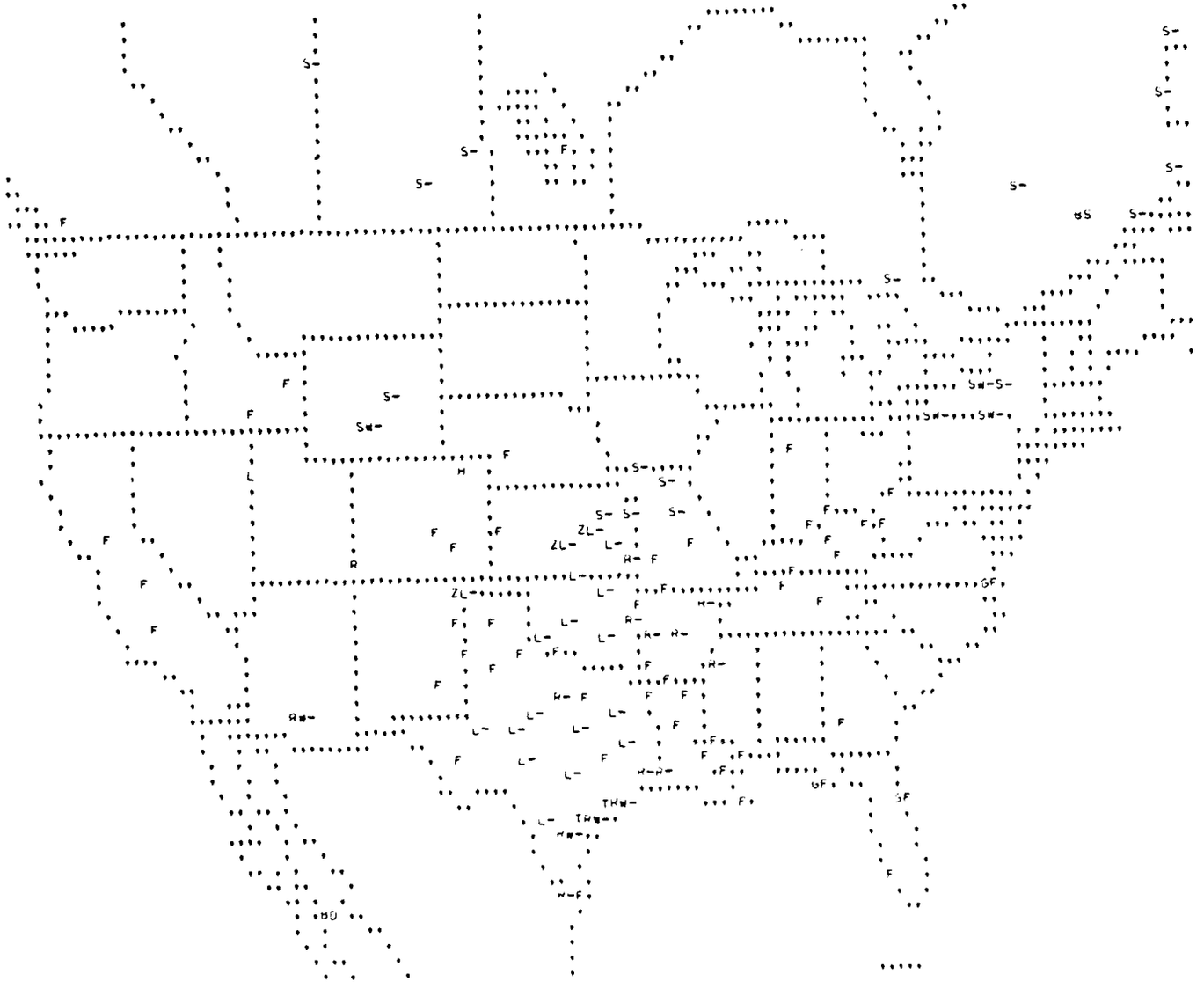

Figure D-1. Line printer plot of current weather.

Figure D-2. Line printer plot of surface temperature.

Figure D-3. Line printer plot of radiosonde station identifiers.

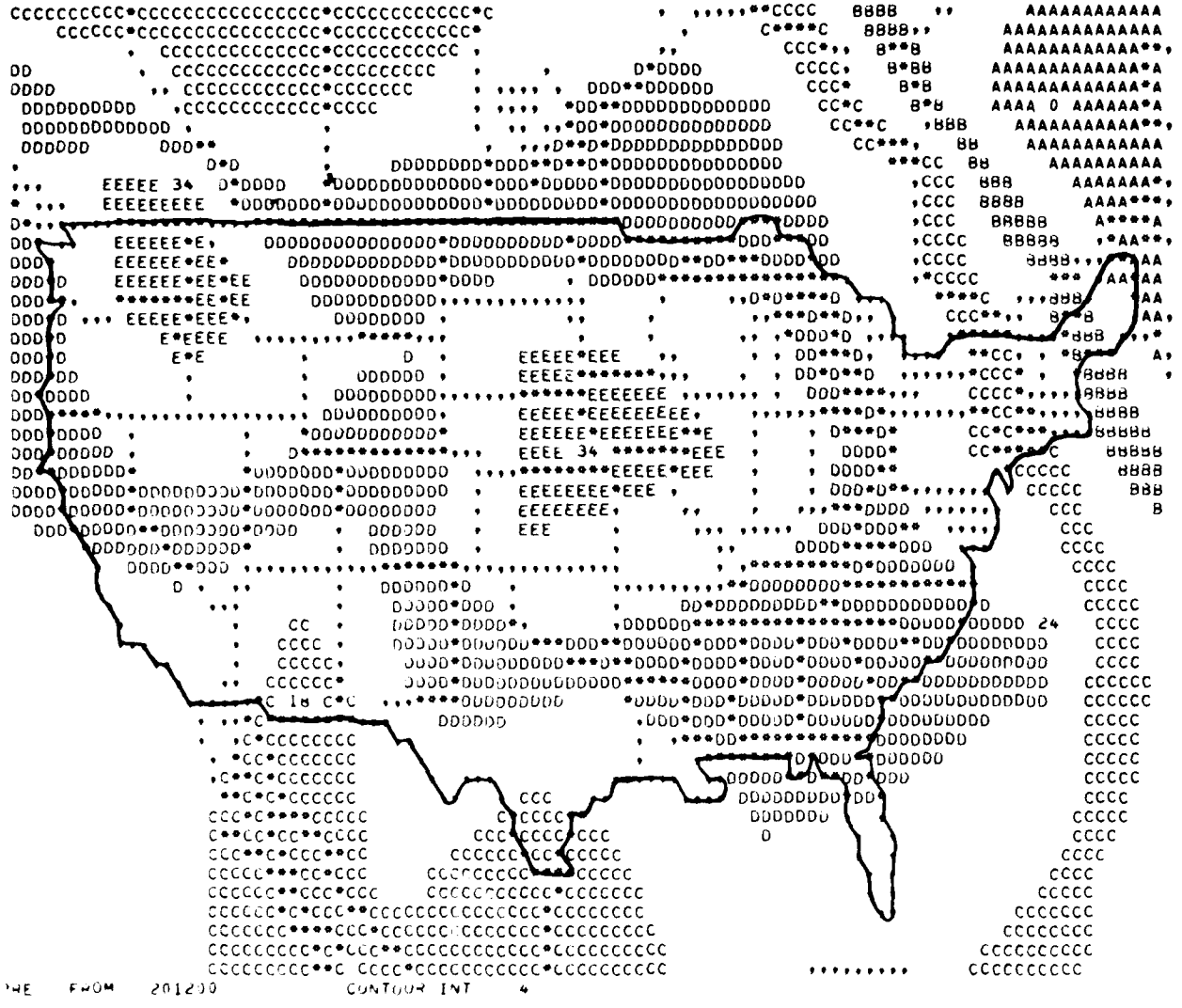

Figure D-4. Line printer analysis of surface pressure over the United States.

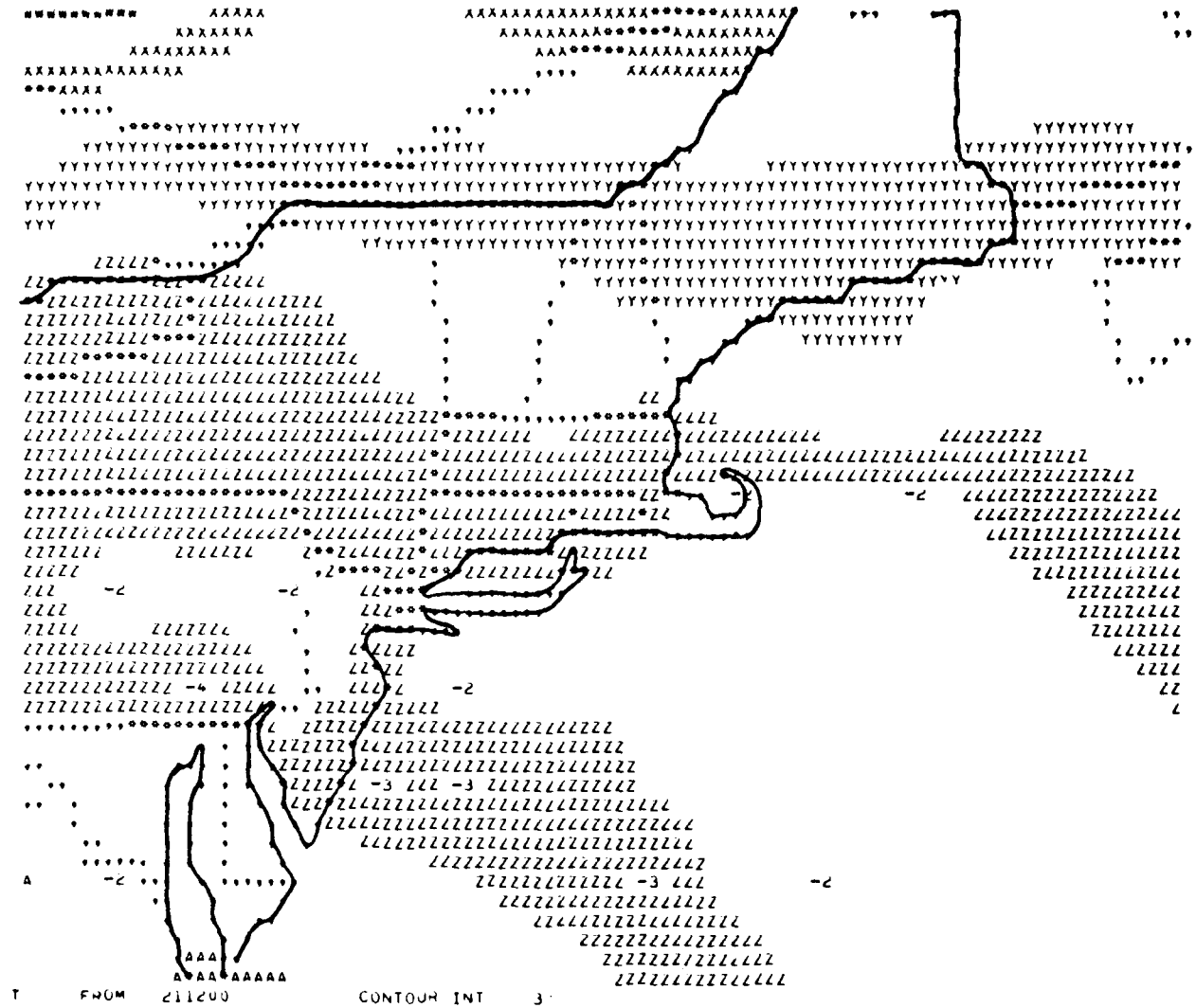

Figure D-5. Line printer analysis of temperature over New England.

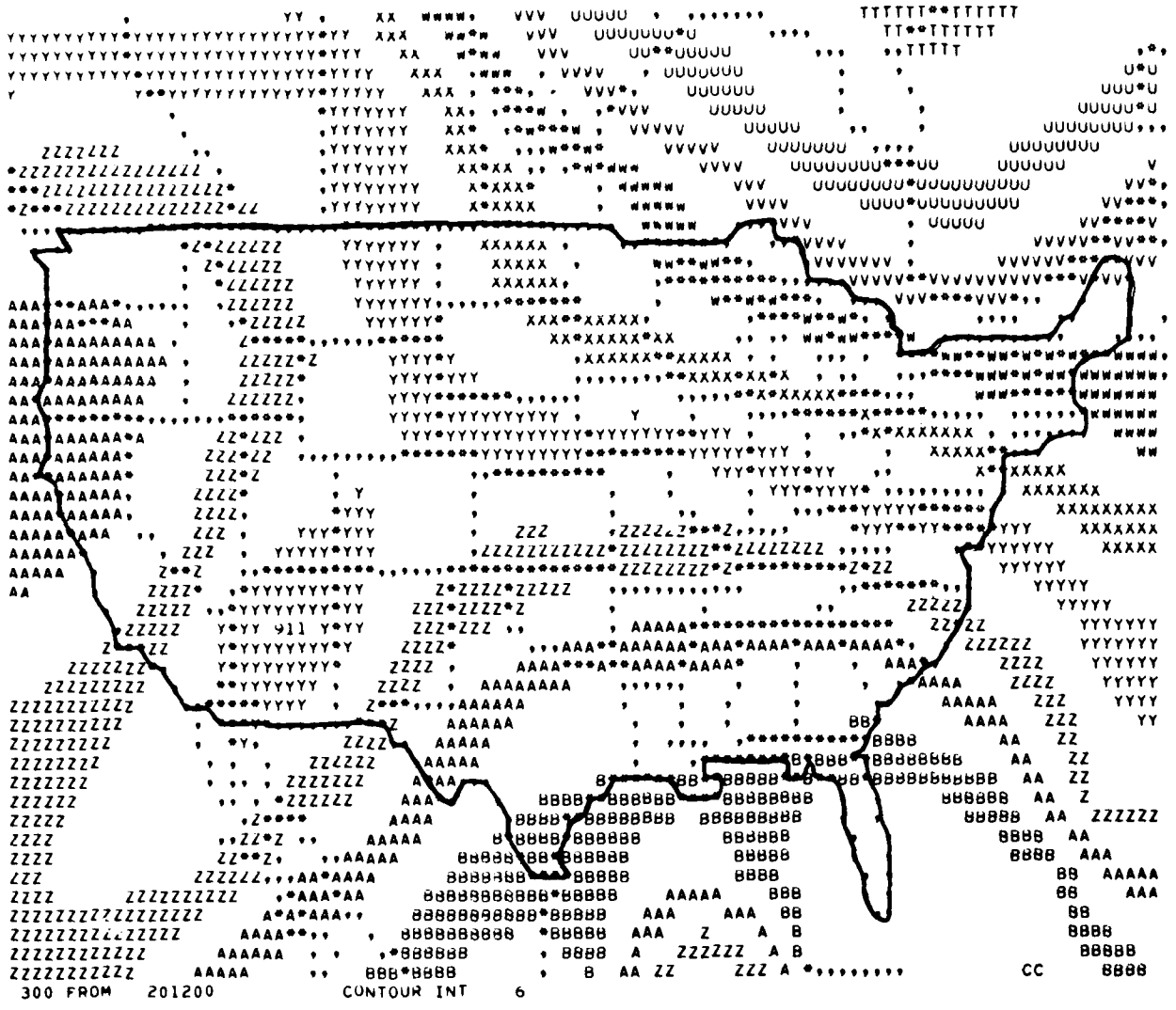

Figure D-6. Line printer analysis of 500 mb heights.

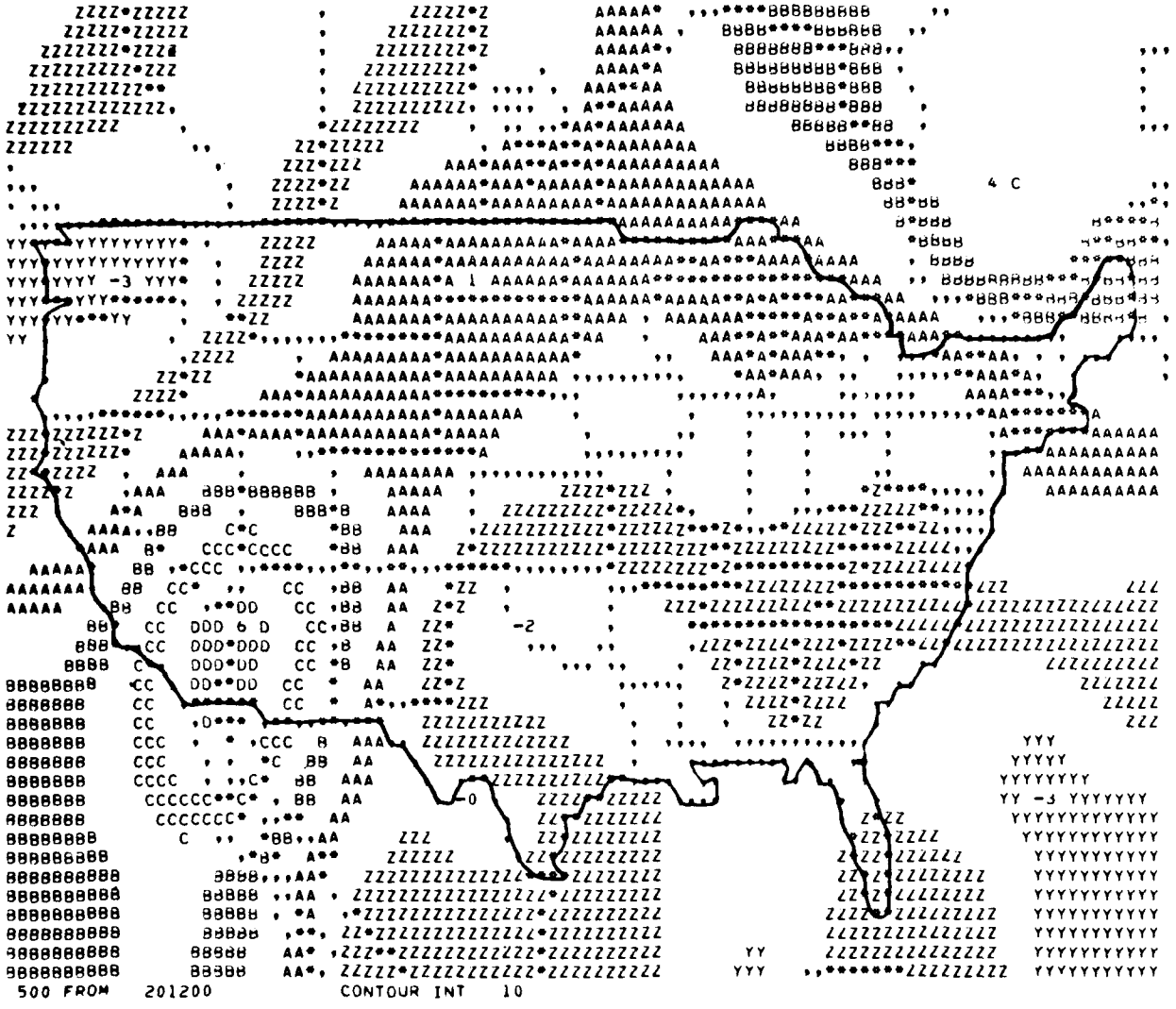

Figure D-7. Line printer analysis of 500 mb vorticity.

```
   ***     A F G L   M C I D A S      ***      PROGRAM:  RAOBDI     TERMINAL: 022  PROJECT:    1006  DATE:   80019  TIME:  192927
   72637  181200
984   2.2     .6 250004   233     748  -2.8 -32.8 270021  2439     422 -32.3 -62.3 245037  6707     224 -45.5       243042 10944
980   1.7     .2 255005   304     735  -1.9 -31.9 270021  2580     400 -35.7 -65.7 245038  7094     212 -46.3       240047 11280
943   -.6   -1.7 275011   609     720  -2.9 -32.9 270020  2743     373 -39.3 -69.3 244038  7576     200 -47.5       235044 11696
908  -2.9   -3.6 280012   914     700  -4.5 -34.5 270019  2966     321 -48.3       242040  8584     195 -48.5       235044 11863
873  -5.3   -5.5 285012  1219     640 -10.4 -40.4 260017  3658     308 -48.3       241041  8856     168 -46.1       240043 12849
864  -6.1   -6.1 285012  1308     591 -15.6 -45.6 250015  4268     300 -49.7       240042  9029     150 -49.7       245041 13597
850  -5.7   -5.7 285013  1436     544 -20.8 -50.8 255015  4878     293 -50.5       240043  9183     116 -56.0       235030 15243
833  -5.1   -5.1 285013  1595     531 -22.5 -52.5 252015  5063     256 -49.5       235051 10060     105 -58.3       235029 15853
823  -6.9  -36.9 285013  1690     522 -23.1 -53.1 250016  5182     250 -49.3       240048 10221     100 -59.7       235029 16188
808  -6.2  -36.2 285014  1829     500 -24.9 -54.9 250022  5502     237 -49.7       243041 10571
777  -4.5  -34.5 275019  2134     460 -27.1 -57.1 248029  6105     233 -48.6       245038 10670
   72528  181200
992   2.8    -.1 240008   224     807     .6 -29.4 245023  1865     546 -14.7 -44.7 254027  4908     237 -50.0       250052 10670
982   2.1    -.4 240009   304     780     .5 -29.5 245025  2134     465 -24.2 -46.5 240030  6097     221 -51.7       247046 11134
945   -.6   -1.9 240013   609     751     .3 -29.7 250023  2439     427 -29.1 -47.4 240029  6707     196 -48.2       240036 11890
909  -3.5   -3.5 240013   923     748     .2 -29.8 250023  2473     375 -36.5 -48.8 240037  7621     180 -45.3       241040 12485
875  -5.4   -5.4 240014  1219     723  -2.0 -32.0 250023  2743     365 -38.1 -49.1 240038  7808     149 -51.8       245050 13719
862  -6.3   -6.3 240015  1341     700  -4.1 -34.1 250023  3000     299 -46.8 -84.6 245046  9146     117 -60.1               15259
850  -5.3   -5.3 240017  1451     643  -9.5 -39.5 255024  3658     275 -50.5       248052  9703
844  -1.3  -31.3 240017  1507     607 -13.3 -43.3 258025  4104     268 -47.3       248054  9872
810     .4 -29.6 245023  1829     594 -13.5 -43.5 260026  4268     260 -47.9       250057 10060
   72518  181200
013   2.0   -5.0 170005    88     817     2.4 -27.6 251010  1820     454 -24.5 -26.3 238031  6349     190 -47.4       245034 12195
000   1.8   -4.2 170005   192     785     2.4 -27.6 245014  2134     432 -26.3 -28.4 235030  6707     182 -43.5       249040 12499
986    .8   -3.8 175007   304     762     2.4 -27.6 245014  2382     400 -29.3 -31.7 245039  7262     166 -46.9       260053 13109
973   -.3   -3.4 190006   412     756     2.0 -28.0 245015  2439     380 -32.2 -35.1 250042  7621     150 -50.7       265025 13778
955   1.2    1.2 212005   562     728     -.1 -30.1 245017  2743     344 -38.1 -41.8 250045  8319     144 -52.6       260021 14024
949   1.2    1.2 220004   609     700    -2.5 -32.5 245018  3061     304 -45.9       250049  9146     121 -61.3       257027 15143
923    .8     .8 260005   836     648    -6.3 -36.3 255017  3658     300 -46.9       250050  9243     113 -62.0       255030 15548
914   1.0    1.0 275006   914     599 -10.2 -40.2 250020  4268     250 -54.7       265060 10429     107 -62.5       265030 15853
880   2.0    2.0 275009  1219     553 -14.2 -44.2 245023  4878     240 -53.9       265059 10670     100 -63.5       250031 16319
870   2.4    2.4 269009  1313     500 -19.3 -49.3 245028  5640     219 -51.6       265047 11280
850   1.2    -.7 255009  1501     476 -22.3 -34.3 242030  6003     200 -49.3       245035 11875
837   1.0   -1.1 254009  1625     469 -22.8 -32.2 240031  6097     195 -49.3       245035 12041
   72606  181200
021  -1.7   -1.7 360000    19     772    -.3 -30.3 217013  2277     534 -15.3 -45.3 236018  5162     250 -54.5       275050 10439
000   -.9    -.9 025001   195     766     1.3 -28.2 218013  2340     500 -18.9 -30.9 240021  5655     240 -51.9       273048 10702
983   -.4    -.4 050002   304     756     1.5 -28.5 220011  2439     471 -22.5 -47.1 245025  6097     220 -54.5       267043 11262
943   1.1    1.1 155003   609     736     1.0 -29.0 223011  2661     459 -24.1 -54.1 245025  6285     208 -47.1       263040 11627
932   1.8    1.8 172004   751     726     -.3  -2.3 224011  2771     443 -25.5 -29.4 244025  6543     200 -45.1       260037 11888
911   1.0    1.0 194004   935     700     -.5  -4.2 230013  3063     400 -31.5 -36.1 240027  7275     185 -45.3       263036 12408
874   3.7    3.7 230007  1219     683    -1.5  -5.1 234013  3259     380 -33.7 -38.4 245028  7621     158 -50.7       270033 13414
873   4.2    4.2 224007  1252     649    -4.8  -7.9 245015  3658     334 -39.5 -44.5 253037  8529     150 -52.7       265024 13764
850   4.0    4.0 220011  1498     610    -8.9 -10.2 241016  4147     304 -44.9       260044  9146     141 -55.5       265026 14181
815   3.7    3.7 210013  1829     600    -9.8 -11.3 240017  4268     300 -45.9       260044  9253     125 -57.8       265031 14939
804   3.6    3.6 211013  1900     554 -14.5 -16.9 235018  4878     265 -52.9       270051 10060     119 -58.7       265027 15243
785    .2     .2 215013  2143     542 -15.4 -16.5 236018  5050     257 -54.7       272051 10262     100 -62.1       260022 16336
```

Figure D-8. Radiosonde data listings.

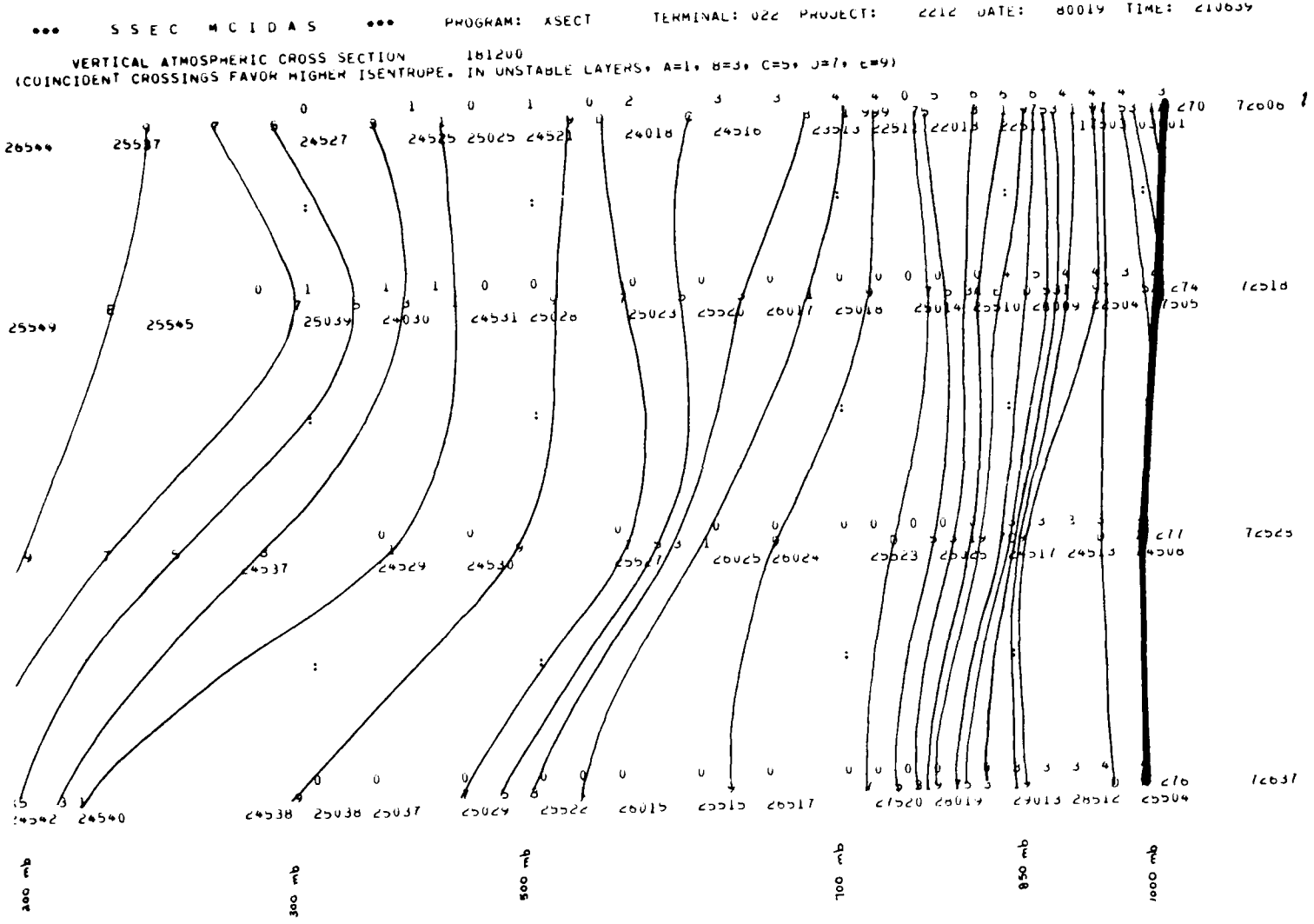

Figure D-9. Vertical cross-section of potential temperature.

printer, data can be listed to facilitate hand plotting (Fig. D-8) or plotted for hand analysis (Fig. D-9).

If the operator indicates a desire to examine conventional data, MFF will lead him through a series of questions and answers until enough information has been elicited for a display to be generated. The operator first chooses the output medium most suited to his needs. Then a choice is made of type of data (surface or upper air) in which he is interested and the form in which it is to be displayed. A specific parameter must be selected for all but those displays representing the entire report for a given station. The time period during which the data were taken, hourly for surface reports and twice daily (0000 and 1200 GMT) for upper air soundings, is then specified. For radiosonde data a quasi-horizontal pressure surface for which the analysis is to be performed is also specified; it must be one of the mandatory reporting levels. The last major option is the map projection as background for the analysis. Choices range from a full U.S. map to regional coverages centered on any of the 50 states. Several additional options are provided for determining color, contour interval, and display format.

In addition to conventional data the chief forecaster may request ingestion of imagery from one of the two geostationary satellites, SMS-2 located off the East coast at 75° West longitude and GOES-3 off the West coast at 135° W. Each satellite transmits full disk imagery at half-hour intervals. SMS-2 image times occur on the hour and half-hour, while GOES-3 begins transmission at 15 and 45 minutes past the hour. In submitting imagery requests the chief forecaster specifies the region of interest, preferred resolution, and image times. Visible and IR data are transmitted simultaneously, so for every image transmission ingested a pair of pictures (one from each channel) is produced, coinciding in spatial and temporal coverage. A series of up to three picture pairs may be requested for this application. The visible sequence is loaded on consecutive TV frames and the IR sequence is loaded on the opposite channel of the analog disk on consecutive frames.

Images may then be examined individually or as short movie loops. It is also possible to study satellite and conventional surface data simultaneously by overlaying analyzed surface reports on the imagery (Fig. C-8).

After completing his examination of current weather information the chief determines the forecast assignment for the day. He selects a surface reporting station as the forecast site and, from the list given in Tab. D-5, three predictands. He also enters the "persistence forecast." He initiates the process with a request, and the actual input of data is performed internally within the program. This function requires retrieval of the most recent hourly surface report submitted by the forecast station and input of the reported values of the three predictands. Persistence assumes that these values will continue to represent actual conditions throughout the forecast period. Persistence will later be used as one standard against which the performance of the forecasters will be judged.

Finally, the chief enters his own forecast. Three predicted values are entered for each predictand. The first is a one-hour forecast, the second verifies in three hours, and the third in six. Multiple forecast lengths were selected to cover a broad range of mesoscale weather phenomena.

B. OPERATIONAL FORECASTER MODULE

The primary function of the operational forecaster module is to allow the participating forecasters to enter their forecasts. Capability to display conventional weather data and satellite imagery is also provided.

All of the conventional data plotting, listing, and analysis options available to the chief forecaster are provided to the operational forecaster. This enables him to check independently those parameters he considers necessary to formulate a forecast but which were not deemed relevant by the chief in the map discussion. The operational forecaster does not have access to the plot file medium, saved commands, or saved displays, since their purpose is to pro-

Table D-5. Predictand Categories

Pred. No.	Predictand	Category 1	Category 2	Category 3	Category 4	Category 5
1	Wind Direction	[1 to 90)°	[90 to 180)°	[180 to 270)°	[270 to 360]°	Null
2	Wind Speed	[0 to 4) kts	[4 to 10) kts	[10 to 20) kts	[20 to 35) kts	[35 to 65] kts
3	Wind Gusts	None	[10 to 20) kts	[20 to 35) kts	[35 to 60) kts	[60 to 120] kts
4	Total Cloud Amount	Clear	Scattered	Broken	Overcast	Null
5	Low Cloud Height	No Clouds	[100 to 1000) ft	[1000 to 2000) ft	[2000 to 3500) ft	[3500 to 6400]ft
6	Middle Cloud Height	No Clouds	[6500 to 12000) ft	[12000 to 17900]ft	Null	Null
7	High Cloud Height	No Clouds	[18000 to 25000)ft	[25000 to 51000]ft	Null	Null
8	Low Cloud Amount	Clear	Scattered	Broken	Overcast	Null
9	Middle Cloud Amount	Clear	Scattered	Broken	Overcast	Null
10	High Cloud Amount	Clear	Scattered	Broken	Overcast	Null
11	Precipitation	Occur	Not Occur	Null	Null	Null
12	Temperature	[-51 to -19)°C	[-19 to -3)°C	[-3 to 3)°C	[3 to 11)°C	[11 to 56]°C
13	Temperature Change	[-40 to -15)°C	[-15 to -5)°C	[-5 to 5)°C	[5 to 15)°C	[15 to 40]°C
14	Visibility	[0 to .2) mi	[.2 to .5) mi	[.5 to 1.) mi	[1. to 3.) mi	[3. to 25.] mi
15	Weather	Occur	Not Occur	Null	Null	Null

[ ] denotes inclusive limit; ( ) denotes exclusive limit

vide easy display of the plot or analysis during the chief's discussion.

The operational forecaster can display the satellite imagery which the chief requested in any manner provided by the facility; i.e., individual frames or visible or IR movie loops. He may also overlay a data plot or surface analysis on the imagery. This capability is limited to existing imagery since no imagery request function is provided by this module.

The forecast entry routine, also provided in the chief forecaster module, comprises the major portion of the operational forecaster module. One option of this routine allows the forecaster to list the forecast station and the three predictands being used that day. A second option initiates the man-machine dialog through which the forecast is entered. Fig. D-10a gives an example of the first option. The station is identified by its three letter Service-A identifier and the predictands are listed in the order in which they appear in the forecast entry dialog.

The second option, the forecast entry dialog, consists of three parts: listing of the last seven surface reports for the forecast station, sample forecast entry, and actual forecast questions.

The first part of the dialog displays the last seven hourly surface reports of the forecast station in chronological order to help the forecaster identify significant trends which will influence his forecast. The forecaster is given the option of having a hard copy of these data should he desire to refer to them later in the dialog. While this display is being prepared the forecast entry routine is calculating the time at which the forecast is being entered and the value of each predictand at that time. These data along with the forecaster's ID are then placed into a buffer that will eventually contain the entire forecast.

The second part of the dialog is a sample forecast entry which familiarizes the forecaster with the data entry format (see Fig. D-10b). Forecast data entered are a set of percent probabilities of occurrence that are assigned to categories which are ranges of values describing the pre-

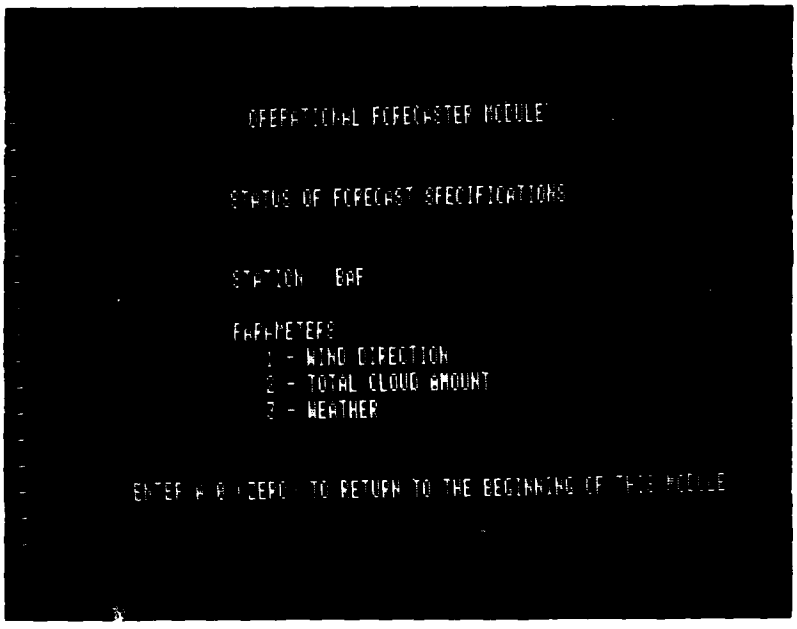

Figure D-10a. "Status of Forecast Specifications" page from the Mesoscale *Forecasting* Facility (MFF).

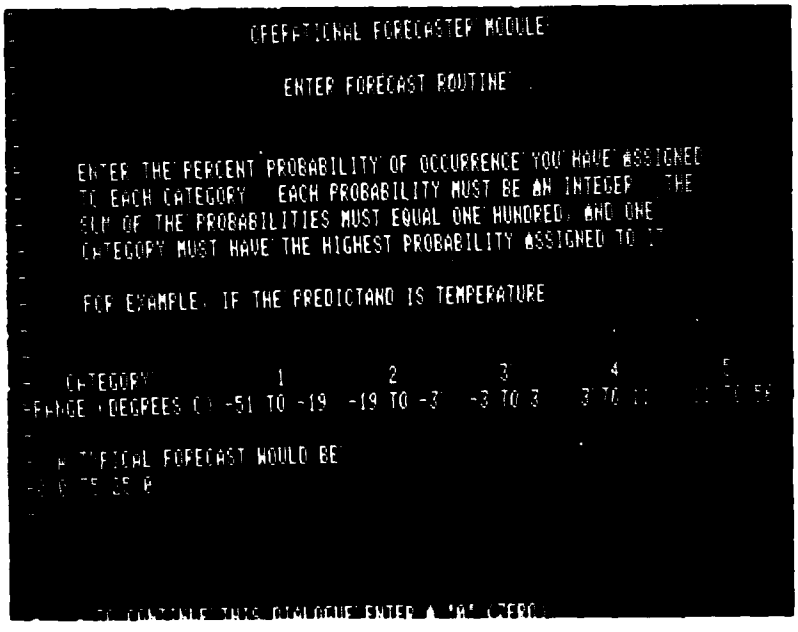

Figure D-10b. Sample forecast entry page from MFF.

dictand. The lone exception to this data format occurs when predictand #15, weather type, is chosen. The forecast entry then consists of a number associated with a weather type and percent probability of its occurrence. (See Tab. D-5 for a listing of categories associated with each predictand, and Fig. D-11b for a list of weather types.)

The sample message begins by describing the restrictions placed on this set of probabilities to allow calculation of meaningful skill scores. These restrictions are: probabilities must be integers in the range $0 \leq x \leq 100$, a single category must have the highest probability assigned to it, and the sum of the probabilities must equal 100.

The remainder of the message displays a typical forecast entry for a sample predictand, temperature. Categories associated with a temperature forecast are listed, followed by the forecast entry:

0 0 75 25 0.

This set assigns a probability of occurrence of 0% to categories 1 and 2, [-51 to -19°C) and [-19 to -3°C); 75% probability of occurrence to category 3 [-3 to 3°C); 25% to category 4 [3 to 11°C); and 0% to category 5 [11 to 56°C].

The weather type forecast would be entered in this form:

47 90

which indicates weather type 47, light freezing drizzle, has a forecasted probability of occurrence of 90 percent.

The third and final part of the forecast entry dialog consists of the questions and answers which build a complete forecast. Fig. D-11a shows a sample forecast question. The display lists forecast station, length of time for which the forecast is being made, forecast time (initial time plus forecast length), and predictand being forecast. This information is followed by a listing of the categories for that predictand. The forecaster then enters a set of probabilities which describes his forecast. The forecast entry routine checks this entry to assure that it meets the restrictions. If it does not, an error message is dis-

Figure D-11a. Forecast entry question from MFF.

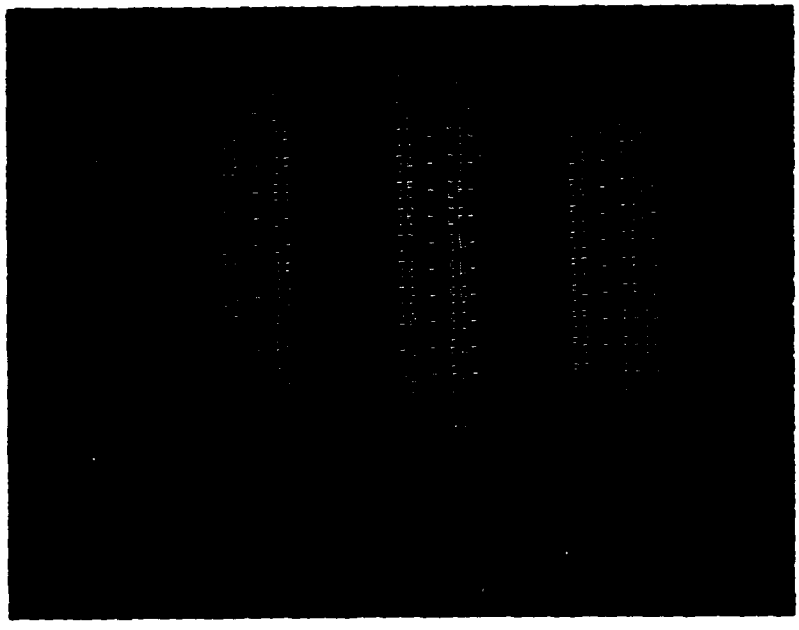

Figure D-11b. Weather types available to forecasters in MFF.

played which identifies the restriction violated and the question is redisplayed. If it meets the restrictions the data are entered into the forecast buffer and the next question is asked. This process continues until an entire forecast has been entered. An entire forecast consists of nine sets of questions and entries, a forecast entry for predictions of 1, 3, and 6 hours for each of the three predictands. When the entire forecast has been entered it is written to a disk file known as the forecast file and the forecast entry dialog is terminated.

C. INTERROGATION MODULE

The function of the interrogation module is to allow the forecaster to review his past forecasts and his forecast skill scores.

In reviewing past forecasts the forecaster is given the option of listing any or all of his five most recent forecasts. Because of space limitations on the forecast file, these are the only ones saved. After he enters his selection, a hard copy of the forecast(s) to be reviewed is produced on the line printer and the interrogation dialog is terminated.

A sample output is shown in Fig. D-12. The output header lists the forecaster's name, three letter ID of the forecast station, and the time the forecast was made in the form MMDDHH where MM is the month, DD is the day, and HH is the hour. The remainder of the listing is divided into nine sections, each consisting of the pertinent data for one forecast length in one predictand. Predictand and forecast length begin the section, followed by the value of the predictand at the time the forecast was made (initial value). The value of the predictand at the verification time (verification value) is then listed if it is available. The probabilities assigned to each category by the forecaster complete the data in one section. The complete listing provides the forecaster with information to determine in a subjective manner whether he made a correct or incorrect forecast.

```
***     A F G L   M C I D A S     ***     PROGRAM:  FORCST
 REVIEW FORECASTS : FORECASTER MIKE E NIEDZIELSKI

STATION: BLV      INITIAL TIME:  13020
PREDICTAND:  T       FORECAST LENGTH:    1 HOURS
INITIAL VALUE :  -7  DEGREES C      VERIFICATION VALUE : MISSING
CATEGORY #  :    1      2      3      4      5
PROBABILITY :    0    100      0      0      0

PREDICTAND:  T       FORECAST LENGTH:    3 HOURS
INITIAL VALUE:   -7  DEGREES C      VERIFICATION VALUE:   -7  DEGREES C
CATEGORY #  :    1      2      3      4      5
PROBABILITY :    0    100      0      0      0

PREDICTAND:  T       FORECAST LENGTH:    6 HOURS
INITIAL VALUE:   -7  DEGREES C      VERIFICATION VALUE:   -8  DEGREES C
CATEGORY #  :    1      2      3      4      5
PROBABILITY :    0    100      0      0      0

PREDICTAND: VIS      FORECAST LENGTH:    1 HOURS
INITIAL VALUE :   1.20  MILES      VERIFICATION VALUE : MISSING
CATEGORY #  :    1      2      3      4      5
PROBABILITY :    0      0      0    100      0

PREDICTAND: VIS      FORECAST LENGTH:    3 HOURS
INITIAL VALUE:    1.20  MILES      VERIFICATION VALUE:     .60  MILES
CATEGORY #  :    1      2      3      4      5
PROBABILITY :    0      0      0     80     20

PREDICTAND: VIS      FORECAST LENGTH:    6 HOURS
INITIAL VALUE:    1.20  MILES      VERIFICATION VALUE:    2.20  MILES
CATEGORY #  :    1      2      3      4      5
PROBABILITY :    0      0      0     20     80

PREDICTAND:  WX      FORECAST LENGTH:    1 HOURS
INITIAL VALUE:  S-       VERIFICATION VALUE: NON
FORECASTED VALUE :  S-
CATEGORY #  :    1      2      3      4      5
PROBABILITY : 100      0

PREDICTAND:  WX      FORECAST LENGTH:    3 HOURS
INITIAL VALUE:  S-       VERIFICATION VALUE:  S-
FORECASTED VALUE :  S-
CATEGORY #  :    1      2      3      4      5
PROBABILITY : 100      0

PREDICTAND:  WX      FORECAST LENGTH:    6 HOURS
INITIAL VALUE:  S-       VERIFICATION VALUE:  S-
FORECASTED VALUE :  S-
CATEGORY #  :    1      2      3      4      5
PROBABILITY : 100      0

        END OF REVIEW OF FORECASTS
```

Figure D-12. Sample output of review of past forecasts.

The review skill scores option allows a more objective method for rating forecasting ability. The forecaster selects the number of predictands he wants to review and then enters the predictands. A hard copy of his skill scores for those predictands is then produced on the line printer and the interrogation dialog is terminated.

A sample output is shown in Fig. D-13. The output is divided into sections according to predictands and forecast lengths similar to the review of past forecast output. Each section is identified by predictand and forecast length. This is followed by the number of forecasts made for that predictand and forecast length, and the actual skill scores. These scores are a P-score, cumulative skill score, Allen utility score, percent correct skill score, and Air Weather Service skill score. Biases applied to each category when calculating these scores are then listed, completing one section of data. The forecaster can use these scores to chart improvement or decline in his forecasting ability.

D. VERIFICATION MODULE

The fourth component of MFF is the verification module, whose function is to verify the forecasts on the forecast file and calculate individual forecaster skill scores. This module is invisible to the user since once initiated it requires no further terminal inputs to perform its function.

When initiated the verification module searches the forecast file for forecasts which have not been verified. Encountering such a forecast, the routine retrieves the actual values of the predictands at the forecast times and incorporates those data into the sector of the forecast file containing the unverified forecast. This process is continued until all forecasts on the file have been verified. Then the probabilities which comprise each individual's forecast are compared with the verification value or a verified persistence forecast, to calculate a P-score, Air Weather Service skill score, Allen utility score, and a percent correct skill score. A cumulative skill score for

```
***     A F G L   M C I D A S     ***     PROGRAM:  FORCST
SKILL SCORE REVIEW : FORECASTER MIKE E NIEDZIELSKI

     PREDICTAND:  WX     FORECAST LENGTH:   1  HOURS

          NUMBER OF FORECASTS MADE:      2
          P-SCORE:  0.00000
          CUM SKILL SCORE:     0.00000
          ALLEN UTILITY SCORE:     1.000
          PER-CENT CORRECT: 100.00000
          AWS SKILL SCORE UNDEFINED
          BIAS:  CATEGORY  1  :    -.02500
          BIAS:  CATEGORY  2  :    0.00000



     PREDICTAND:  WX     FORECAST LENGTH:   3  HOURS

          NUMBER OF FORECASTS MADE:      2
          P-SCORE:  1.00000
          CUM SKILL SCORE:      .50000
          ALLEN UTILITY SCORE:      .500
          PER-CENT CORRECT:  50.00000
          AWS SKILL SCORE UNDEFINED
          BIAS:  CATEGORY  1  :     .95000
          BIAS:  CATEGORY  2  :    -.95000



     PREDICTAND:  WX     FORECAST LENGTH:   6  HOURS

          NUMBER OF FORECASTS MADE:      2
          P-SCORE:  0.00000
          CUM SKILL SCORE:     0.00000
          ALLEN UTILITY SCORE:     1.000
          PER-CENT CORRECT: 100.00000
          AWS SKILL SCORE:  1.00000
          BIAS:  CATEGORY  1  :    -.02500
          BIAS:  CATEGORY  2  :    0.00000
```

Figure D-13. Sample output of review of skill scores.

all the individual's forecasts for each predictand and forecast length is also calculated, and the category biases for doing these calculations are updated. This process is repeated for each forecaster ID on the forecast file. Then a message indicating completion of verification is displayed and control is returned to the beginning of the MFF program.

E. IMPROVEMENT OF BRIGHTNESS ANALYSIS TECHNIQUE

I. INTRODUCTION

Use of geostationary satellite data to provide information regarding cloud cover and significant weather requires the development of algorithms to discriminate between the earth's surface and cloud type and amount in the automatic processing of satellite imagery. SASC advances in this area are the subject of this section.

II. DATA SAMPLE

Data to be analyzed by the processing software consist of hourly visible and infrared imagery for the northeastern U. S. as received from two geostationary satellites (GOES I and GOES II). The region covered corresponds to 500 visible scan lines, each consisting of 765 picture elements or pixels of one-mile resolution brightness counts. The IR imagery consists of 125 scan lines each containing 896 pixels of four-mile resolution thermal counts. The IR sensor samples every two miles (at the subpoint) along the scan line, resulting in twice as many pixels in the east-west direction as in the north-south direction.

One hour's data are preceded by a header record containing Greenwich Mean Time, first and last line numbers of the IR rows recorded, and the number of the first element in the visible lines to be recorded. These row and element numbers are based on their location in a full disk picture of the earth. The data sample is divided into 125 sets consisting of four visible data lines, one per record, and one record of IR data. Each visible scan line record is preceded by a standard identification word. The IR record also contains 128 words of data which describe the Greenwich Mean Time at which the scan occurred, Julian date, line number, and other information

not relevant here. Each count value is an 8-bit byte and is recorded as part of a 24-bit word. Each tape contains a maximum of 24 images, usually for the six to eight hours when the sun provides sufficient illumination; i.e., local afternoon.

Location of any point in the longitude-latitude coordinate system can be expressed in the line-element coordinate system through the use of a navigation transform based on the full earth disk image scanned by the satellite and known orbital parameters. Line and element numbers of four standard locations within the data area (46°N, 83°W, and the FAA reporting stations at Bedford, Mass., Block Island, R.I., and Dulles International Airport, Va.) are used as input data for reference points to locate any other point in the data area.

III. SOFTWARE DESCRIPTION AND DEVELOPMENT

Data processing software consists of four parts: 1) station locating routine (program CENTER) which retrieves imagery data for a particular area from the data tape; 2) bit manipulating routine (subroutine EIBYT) to convert the 24-bit word format of the data tape to the 60-bit word format of the analyzing hardware; 3) data normalizing routine (subroutine NORMAL) to correct missing or garbled data; and 4) data analyzing routine (subroutine BRIGHT).

CENTER calculates the row and element number of the station for each hour to be analyzed. The data buffer is then filled with the brightness value of each pixel in an array of 7,200 elements (120 rows by 60 elements) using the station row and element as the center and the line number associated with each row of data. The large size of this array insures an adequate sample for the normalizing routine to function properly. While each row of data is being entered into the array, EIBYT is converting the 24-bit data words containing three 8-bit brightness values into 60-bit words containing one brightness value.

This process is necessary to resolve the data structure differences between the archiving hardware (McIDAS) and the analyzing hardware (CDC 6600). The data buffer is then passed to NORMAL and BRIGHT for normalization and analysis. Upon completion of analysis the data tape is advanced to the next hour's data, the reference point relocated, and the process is repeated, until all hours on the tape have been analyzed.

In an effort to increase the amount of analysis done during each run of the data tape, CENTER was modified to calculate the line and element number of up to five stations. The number of lines between the station being analyzed and the next station on the list can be determined algebraically. This allows the tape to be advanced or rewound the appropriate number of lines so as to be positioned at the beginning of the 120 lines of data centered on the new station. In this fashion several stations can be analyzed before the tape is advanced to the next hour, thus increasing the amount of analyzed data per run as much as five times.

Since some data are inevitably lost or garbled in transmission from the satellite, NORMAL was developed to normalize or correct them. Normalization begins by calculating the average of each of the 120 lines of data. If a line average differs by more than 20 from the preceding line average, that line is flagged to indicate that it contains garbled or noisy data. To prevent comparing a line average to the average of a garbled line of data, the average of a noisy line is replaced by the average of the last good line of data encountered. After all lines in the sample have been tested, noisy lines are replaced element for element by the average of corresponding elements in the two adjacent good lines of data.

The final step involves isolating the 27 lines of data which will be processed by the analyzing routine. This is done by calculating the line number of the thirteenth line of data before the station row. This line and the next 26 lines of data are then copied onto a temporary disk file to be passed to BRIGHT for analysis.

Several modifications were made to this routine to reduce processing time and increase data integrity. First, the line numbers of the 27 lines of data to be analyzed are checked to insure that they are consecutive lines. The original normalizing process ignored missing lines by merely taking the first 27 lines of date it encountered which had line numbers greater than or equal to the initial row number of the sample set to be analyzed. The modified routine can detect non-consecutive line numbers and calculate the number of imbedded blank lines. These lines are filled with dummy brightness values and flagged as being noisy. The process of isolating the 27 line set was shifted to occur before the replacing of noisy lines takes place. This allows blank lines to be filled with normalized data and also allows the routine to replace noisy lines within the data sample to be analyzed without having to do it for the entire 120 line normalizing sample. To further reduce normalizing time, the use of a scratch disk file to hold the normalized data and its attendant input-output was eliminated by placing only the 27 elements of each of the 27 lines of data to be analyzed into a common block of storage within the program. This provides instant program access without the need for time-consuming reading from or writing onto a scratch file.

After the data have been normalized and isolated the analysis routine BRIGHT begins processing. The 27 x 27 array is divided into nine 9 x 9 blocks, as shown in Fig. E-1a, and each of these blocks is further subdivided into 3 x 3, 5 x 5, 7 x 7, and 9 x 9 pixel boxes (see Fig. E-1b) for analysis purposes. Average brightness, standard deviation, and the range of values for each box are calculated and the maximum and minimum brightness value in each are determined. The brightness value of the central pixel of these nested boxes is noted and the gradient from each edge to the center is calculated for all four boxes.

These analyses are performed for each of the nine blocks and for the entire 27 x 27 array. A sample output of the analysis is shown in Fig. E-2. The first two

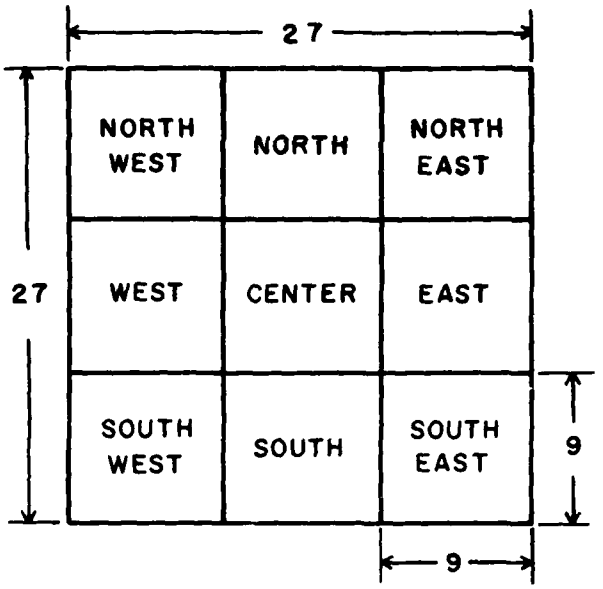

Figure E-1a. Divisions of the 27x27 array. Dimensions are in pixels.

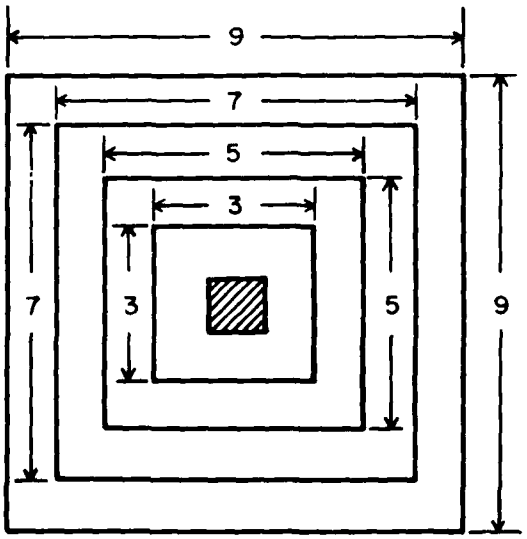

Figure E-1b. Nested boxes within a 9x9 block. Shaded area is central pixel. Dimensions are in pixels.

[illegible] 7431, VID EL SKIP= 415, CORRECT FR J E= 2 *--1600,0259,0364,13,1905.----------

[illegible] AVERAGE AND STANDARD DEVIATION CENTERED ON SYRACUSE — 9 X 9 BLOCKS 30 MAR 77

NORTH

BLOCK	ONE	TWO	THREE	FOUR
AVG	76	75	75	75
SD	1.4	2.8	3.1	3.1
MAX	78	79	80	82
MIN	74	64	64	64
RANGE	4	15	16	18
DIFFERENCE TO CENTER	78			
WEST	0	0	0	-2
EAST	2	4	2	4
NORTH	-1	-3	0	-2
SOUTH	2	3	3	0

NORTHEAST

BLOCK	ONE	TWO	THREE	FOUR
AVG	71	71	71	72
SD	1.8	2.3	3.9	4.7
MAX	74	75	80	84
MIN	68	67	63	63
RANGE	6	8	17	21
DIFFERENCE TO CENTER	70			
WEST	4	2	2	6
EAST	0	-2	0	-2
NORTH	3	3	2	6
SOUTH	-2	-1	5	4

WEST

BLOCK	ONE	TWO	THREE	FOUR
AVG	77	76	76	76
SD	2.3	2.3	2.4	2.6
MAX	81	81	82	82
MIN	74	73	73	72
RANGE	7	8	9	10
DIFFERENCE TO CENTER	76			
WEST	0	0	2	0
EAST	-4	2	0	-2
NORTH	-2	-3	-3	-4
SOUTH	-1	3	0	-2

CENTER

BLOCK	ONE	TWO	THREE	FOUR
AVG	78	77	77	77
SD	1.4	1.6	1.4	1.6
MAX	80	80	80	80
MIN	75	75	74	72
RANGE	5	5	6	8
DIFFERENCE TO CENTER	78			
WEST	0	-2	0	-2
EAST	-2	-2	0	0
NORTH	-1	-1	-1	-1
SOUTH	1	3	2	2

EAST

BLOCK	ONE	TWO	THREE	FOUR
AVG	76	75	75	75
SD	1.8	2.5	2.9	3.5
MAX	79	80	81	81
MIN	73	71	69	67
RANGE	6	9	12	14
DIFFERENCE TO CENTER	78			
WEST	-2	-2	0	-2
EAST	0	-2	-0	-2
NORTH	-3	-6	-8	-11
SOUTH	3	-1	-2	2

SOUTHWEST

BLOCK	ONE	TWO	THREE	FOUR
AVG	74	74	74	76
SD	6.3	5.3	5.3	5.3
MAX	82	82	84	85
MIN	64	64	56	56
RANGE	18	18	28	29
DIFFERENCE TO CENTER	73			
WEST	8	8	4	8
EAST	6	-2	-2	-2
NORTH	5	0	6	2
SOUTH	-6	-3	-1	-12

SOUTH

BLOCK	ONE	TWO	THREE	FOUR
AVG	79	78	78	78
SD	3.5	3.2	2.9	3.2
MAX	85	85	85	86
MIN	75	73	73	71
RANGE	10	12	12	15
DIFFERENCE TO CENTER	75			
WEST	10	8	4	8
EAST	0	-2	-2	-6
NORTH	3	-1	0	-4
SOUTH	-2	1	-3	-6

SOUTHEAST

BLOCK	ONE	TWO	THREE	FOUR
AVG	77	78	77	77
SD	3.0	3.5	3.2	3.0
MAX	80	86	86	86
MIN	71	71	70	70
RANGE	9	15	16	16
DIFFERENCE TO CENTER	75			
WEST	0	0	2	2
EAST	0	-2	0	0
NORTH	5	5	2	2
SOUTH	-2	-11	-9	0

TOTAL PICTURE 27 X 27

AVG	SD	MAX	MIN	RANGE	DIFF CENTER	WEST	EAST	NORTH	SOUTH
76	3.9	86	56	30	78	-2	2	-2	-3

Figure E-2. Sample brightness analysis output. Values are visual count values based on a 256-count range.

lines of output give the Julian day and Greenwich Mean Time of the data being analyzed, station name, its row and element numbers, and a fine-tuned navigation correction factor which aligns the image coordinates with the earth surface coordinates. The label which precedes the hourly data on the tape is also listed. Analysis of the nine blocks is arranged as shown, followed by analysis of the 27 x 27 array. A final line indicates the number of blank lines of data in the analysis sample. This is included to provide a basis for accepting or rejecting the analysis. All of these output values are also sorted by station and written to separate permanent files for future reference and further analysis.

To augment this brightness value analysis and eliminate data dependency on varying solar elevation angles, routine ALBEDO was written to convert brightness analysis results to their corresponding albedo values. It was decided to perform this task using a separate routine to keep CENTER running time to an absolute minimum. The maximum, minimum, central, and range of values for brightness data can be converted to albedo values by using the formula:

$$A = (B/C)^2 \ (1/\cos Z)$$

where A is albedo value, B is corresponding brightness value, C is a constant equal to 234 for GOES I and 255 for GOES II data, and Z is solar zenith angle. Z is calculated by a separate routine using Julian day, Greenwich Mean Time, and longitude and latitude of the station.

The average and standard deviation conversion was more involved since:

$$\bar{A} = \sum (B/C)^2 \ (\tfrac{1}{N})(1/\cos Z)$$

and $$\sigma_A = \left\{ \sum \left[(B/C)^2 \ (1/\cos Z) \right]^2 / N - \bar{A}^2 \right\}^{\frac{1}{2}}$$

and $\sum B^2$ and $\sum B^4$ are not directly calculated by BRIGHT and included in the output data. $\sum B^2$ can however be determined from the equation:

$$\sigma_B = \left[\sum B^2 / N - \bar{B}^2 \right]^{\frac{1}{2}}$$

since σ_B and $\bar{B}$ are known values. N can be calculated from the analysis box size. Only σ_A cannot be calculated from data output by BRIGHT. This was corrected by adding $\sum B^4$ to the values calculated in that routine and saved on the output file. Gradient analyses were omitted from the albedo analysis because no new information could be obtained from them in albedo form.

Output format for albedo analysis (Fig. E-3) is similar to the brightness analysis. Use of brightness and albedo data provides a basis for discriminating between surface brightness and clouds.

Efforts to include infrared data analysis in CENTER have begun. Differences between one-mile resolution brightness data and four-mile IR data have been reconciled by dividing each IR pixel into 8 pixels of the same value. These expanded IR data are then aligned with the brightness data to produce a one-to-one correspondence betweeen brightness or visible data pixels and IR pixels. Brightness analysis software can then be used on IR data. Difficulties in normalizing IR data have thus far prevented sustained analysis.

IV. CONCLUSIONS

Improvements in program CENTER have increased efficiency of execution time and reliability of results. Run time per station analyzed has been reduced 62 percent and field length requirement has been halved, resulting in a 32 percent cost saving per station analyzed. Incomplete data samples can be identified and rejected on the basis of the number of blank lines of data, removing a source of erroneous results in later analyses. The addition of albedo analysis has increased the data base for ground/cloud discrimination.

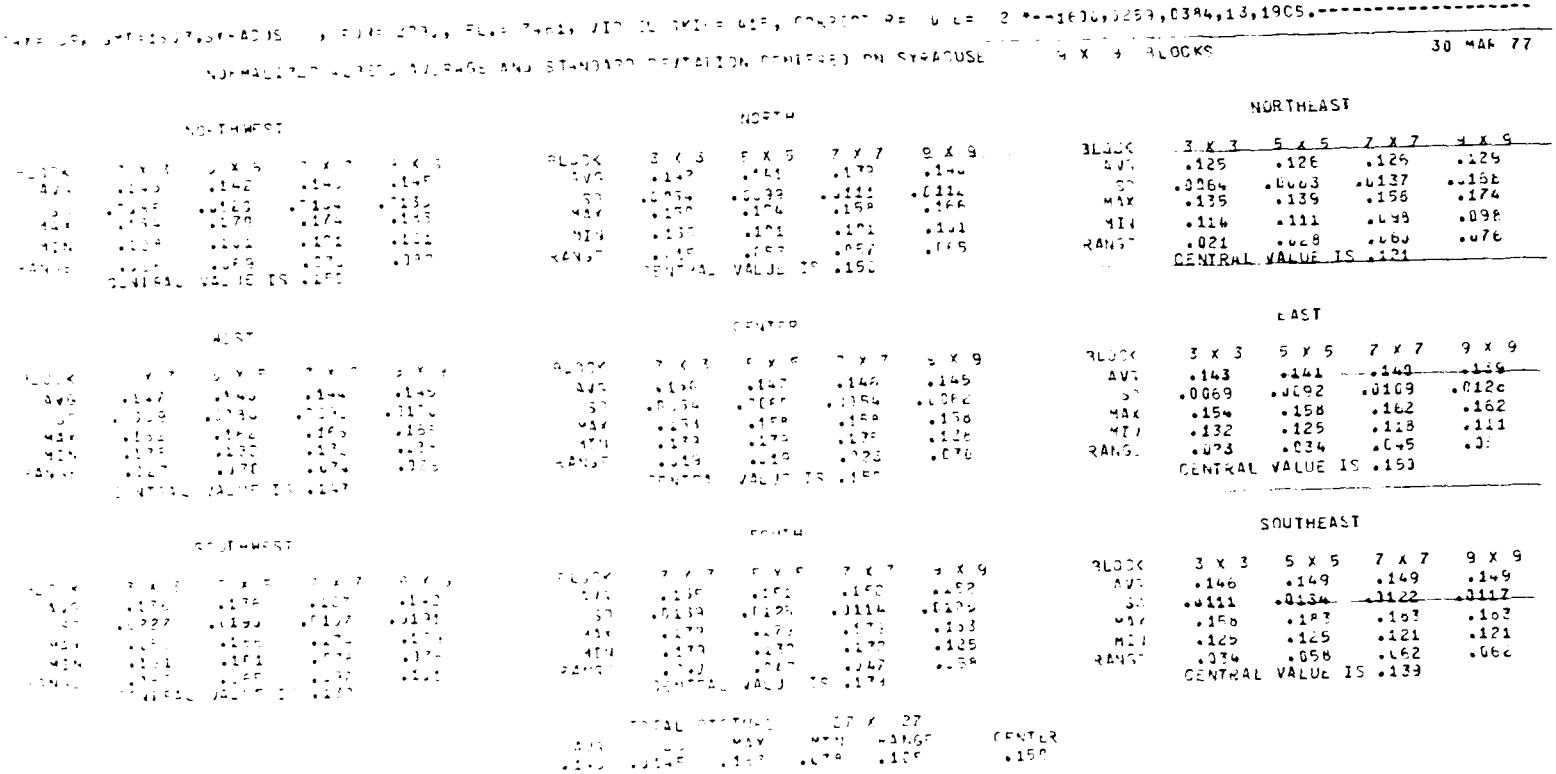

NORTHWEST

BLOCK	3 X 3	5 X 5	7 X 7	9 X 9
AVG	.143	.142	.144	.145
SD	.0056	.0049	.0111	.0114
MAX	.150	.154	.158	.158
MIN	.137	.131	.131	.131
RANGE	.013	.023	.027	.027

CENTRAL VALUE IS .150

NORTH

BLOCK	3 X 3	5 X 5	7 X 7	9 X 9
AVG	.143	.141	.139	.140
SD	.0056	.0049	.0111	.0114
MAX	.150	.154	.158	.158
MIN	.137	.131	.131	.131
RANGE	.013	.023	.027	.027

CENTRAL VALUE IS .150

NORTHEAST

BLOCK	3 X 3	5 X 5	7 X 7	9 X 9
AVG	.125	.126	.126	.126
SD	.0064	.0063	.0137	.0161
MAX	.135	.139	.156	.174
MIN	.114	.111	.098	.098
RANGE	.021	.028	.060	.076

CENTRAL VALUE IS .121

WEST

BLOCK	3 X 3	5 X 5	7 X 7	9 X 9
AVG	.147	.146	.144	.145
SD	.0059	.0056	.0094	.0096
MAX	.156	.156	.162	.162
MIN	.135	.135	.132	.132
RANGE	.021	.021	.030	.030

CENTRAL VALUE IS .147

CENTER

BLOCK	3 X 3	5 X 5	7 X 7	9 X 9
AVG	.136	.142	.146	.145
SD	.0054	.0065	.0064	.0062
MAX	.144	.150	.158	.158
MIN	.123	.129	.135	.128
RANGE	.021	.021	.023	.030

CENTRAL VALUE IS .150

EAST

BLOCK	3 X 3	5 X 5	7 X 7	9 X 9
AVG	.143	.141	.140	.139
SD	.0069	.0092	.0109	.0126
MAX	.154	.158	.162	.162
MIN	.132	.125	.118	.111
RANGE	.023	.034	.045	.051

CENTRAL VALUE IS .150

SOUTHWEST

BLOCK	3 X 3	5 X 5	7 X 7	9 X 9
AVG	.136	.136	.136	.136
SD	.0077	.0092	.0107	.0111
MAX	.144	.144	.144	.144
MIN	.121	.121	.121	.121
RANGE	.023	.023	.023	.023

CENTRAL VALUE IS .139

SOUTH

BLOCK	3 X 3	5 X 5	7 X 7	9 X 9
AVG	.135	.131	.130	.132
SD	.0059	.0096	.0114	.0126
MAX	.139	.144	.147	.153
MIN	.129	.120	.117	.125
RANGE	.010	.024	.030	.028

CENTRAL VALUE IS .134

SOUTHEAST

BLOCK	3 X 3	5 X 5	7 X 7	9 X 9
AVG	.146	.149	.149	.149
SD	.0111	.0134	.0122	.0117
MAX	.156	.183	.183	.183
MIN	.125	.125	.121	.121
RANGE	.031	.058	.062	.062

CENTRAL VALUE IS .139

TOTAL REGION 27 X 27

AVG	SD	MAX	MIN	RANGE	CENTER
.140	.0146	.183	.098	.085	.150

Figure E-3. Sample albedo analysis output.

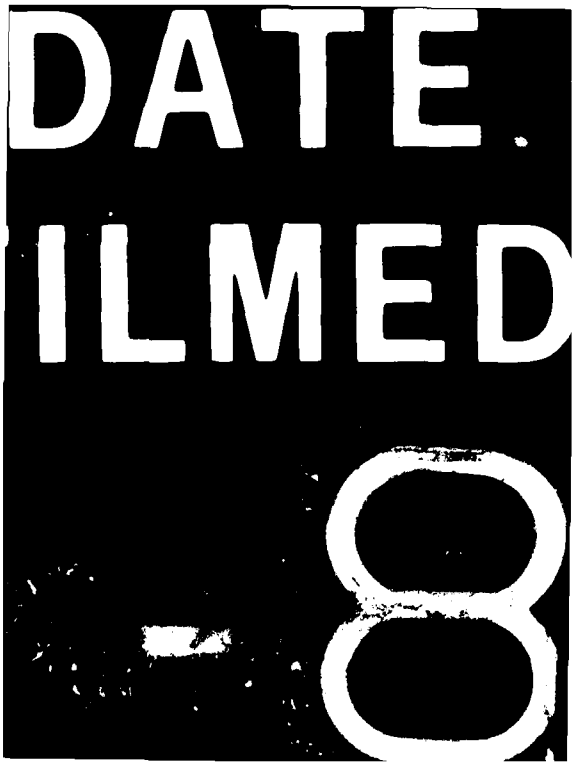
DATE
ILMED
8